FPP alignment in SBS

Andrew Puckett

SBS Weekly Meeting

March 28, 2018

Outline

- Urgent question: final design/procurement of SBS GEM support frame for GEP/GEN recoil polarization—need science-driven specifications:
  - Stability/rigidity
  - Reproducibility/repeatability
  - Absolute Accuracy
- Current frame design does NOT accommodate easy removal/re-insertion of the CH_2 analyzers from the acceptance for collection of "straight-through" calibration data (for alignment of polarimeter GEM chambers with front GEM chambers)
- This is inconsistent with previous practice in Halls A and C, in which C/CH_2 analyzers were easily mechanically removable from acceptance in a short (~30 minutes) controlled access.
- Importance (or lack thereof) of FPP scattering angle reconstruction systematics at high Q^2
- Hall A/C experience
- Can we achieve an adequate software alignment without collecting dedicated straight-through data?
- Hall C FPP alignment study using GEp-III/GEp-2γ data

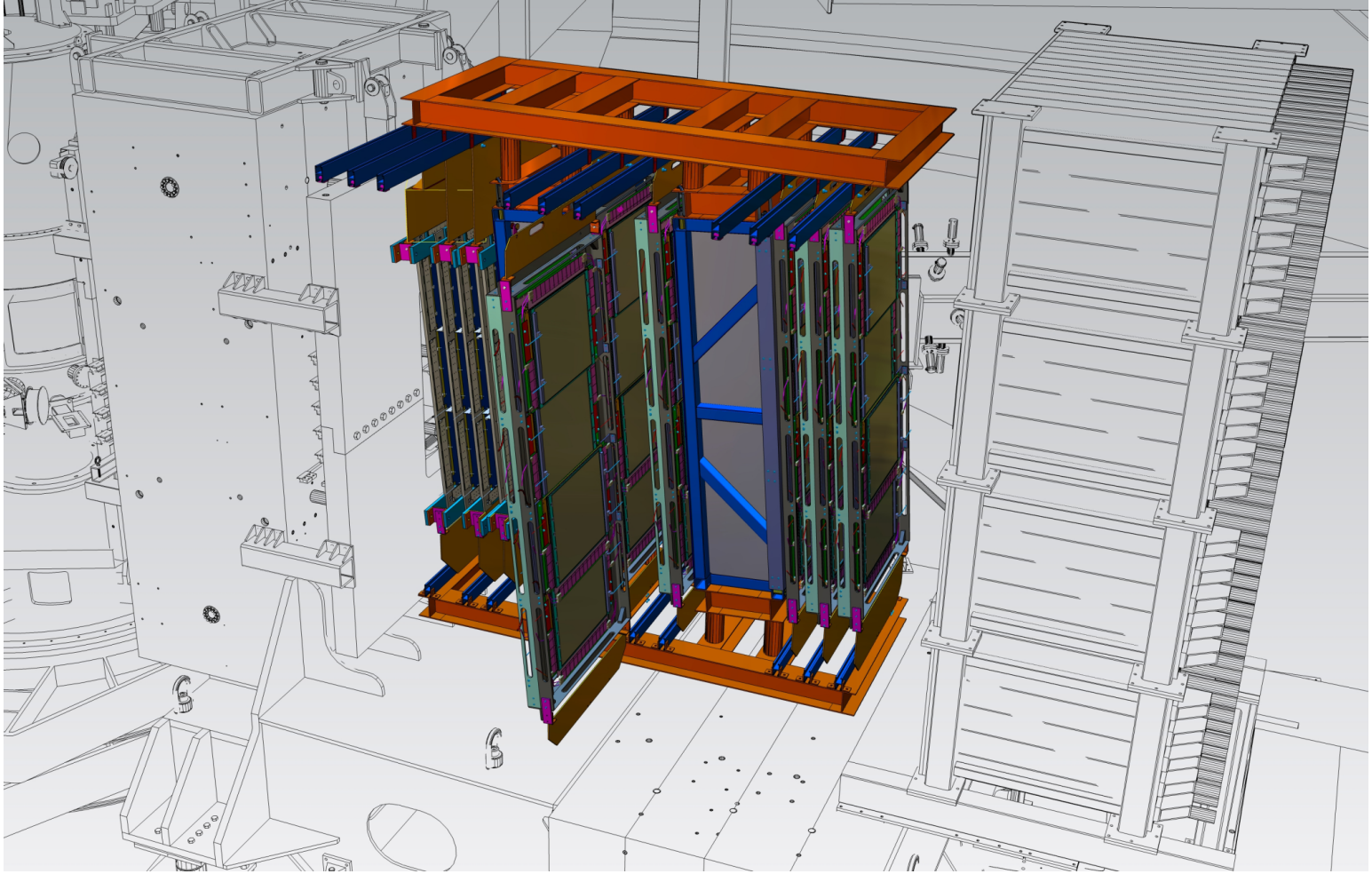

- What absolute accuracy, stability and reproducibility of Front Tracker positioning/orientation is needed for spin transport/optics systematics to be kept to an acceptable level?
- What absolute accuracy, stability, and reproducibility is needed for FPP1/FPP2 trackers to keep FPP angle reconstruction systematics to an acceptable level?
- To the extent that CH_2 is removable, will the removal/reinsertion operation cause the GEM chambers to move, defeating the purpose of straight-throughs?

New Alignment Study of Hall C HMS+FPP data

- Goal: test feasibility of doing "in situ" software alignment of FT+FPP1+FPP2 GEM trackers (SBS) using production data from HMS + FPP1 + FPP2 drift chamber trackers (Hall C)
- Use $Q^2 = 5.2$ GeV^2 and $Q^2 = 6.8$ GeV^2 data (comparable to SBS lower-Q^2 points)

Hall C Focal Plane Polarimeter (FPP)

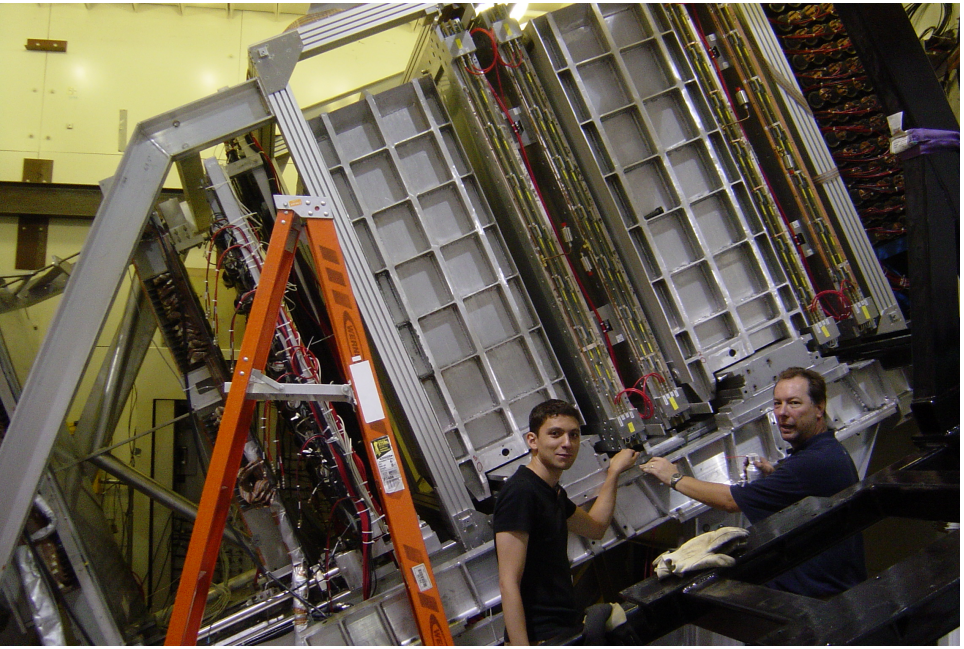

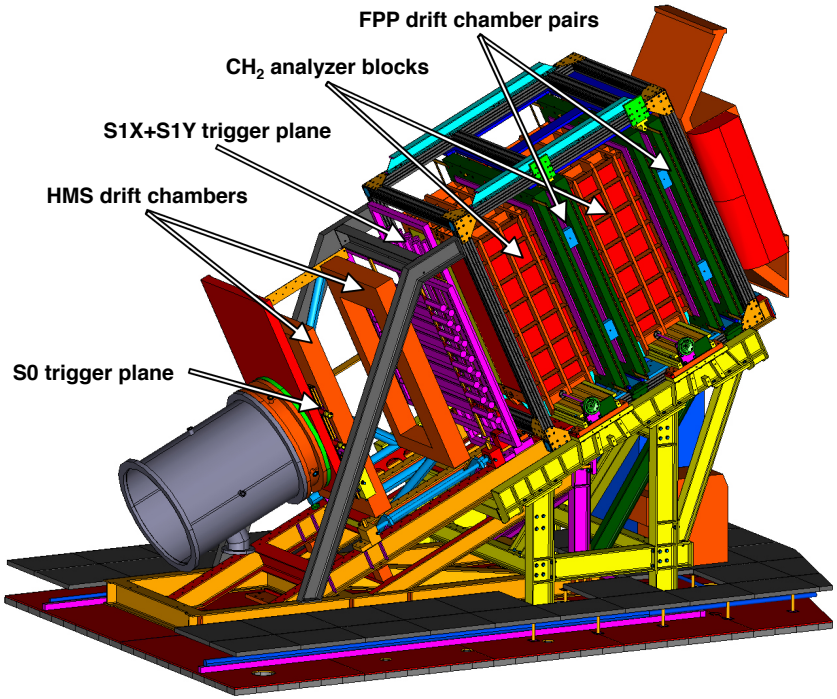

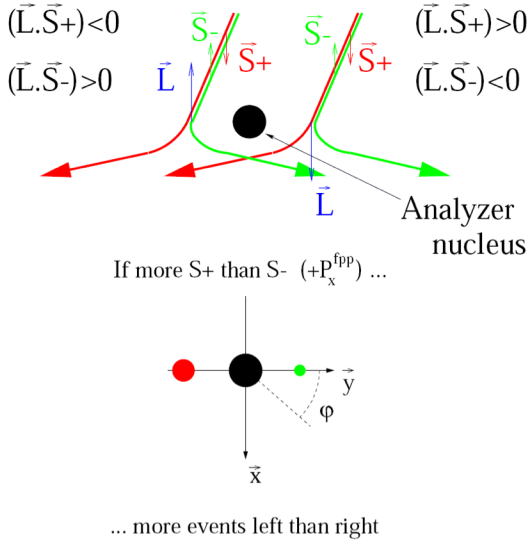

- Proton polarimetry via proton-nucleus scattering is based on the spin-orbit coupling in the nucleon-nucleon force.
- A spin-1/2 particle, such as a proton, is preferentially deflected by a spin-orbit force along the direction of $\vec{p}\times\vec{S}$, where $\vec{p}$ is the incident proton momentum, and $\vec{S}$ is the proton spin.
  - Note that a spin-orbit force is insensitive to longitudinal polarization!
- By tracking the incident and scattered proton and measuring the azimuthal asymmetry in the angular distribution of secondary scatterings, the incident proton's (transverse) polarization can be reconstructed
- Retractable CH_2 analyzers allow collection of "straight-through" data for calibration/alignment

FPP design aspects and motivation

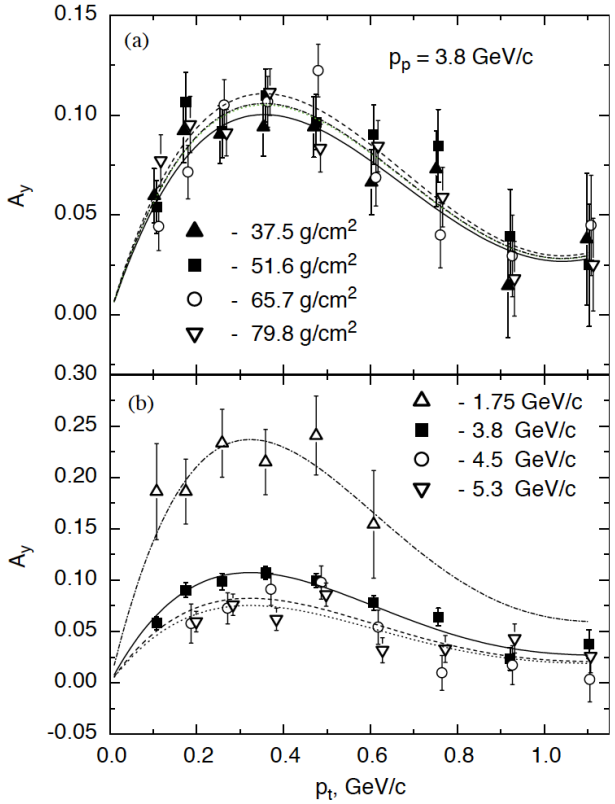

Fig. 4. Analyzing powers as a function of p_t: (a) for different target thicknesses at $p_p = 3.8\,\mathrm{GeV}/c$; (b) for different momenta at $L = 51.6\,\mathrm{g/cm^2}$.

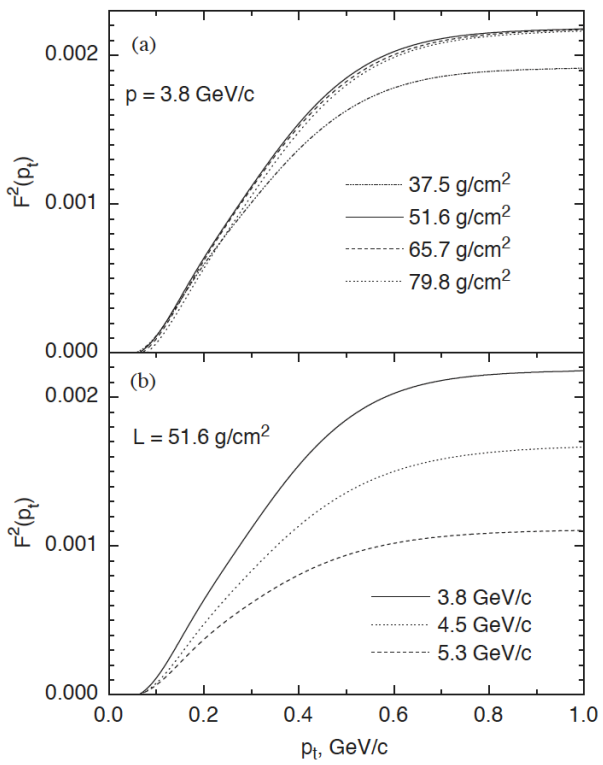

Fig. 6. Figure of merit as a function of p_t: (a) for different target thicknesses at $p_p = 3.8\,\mathrm{GeV}/c$; (b) for different momenta at $L = 51.6\,\mathrm{g/cm^2}$.

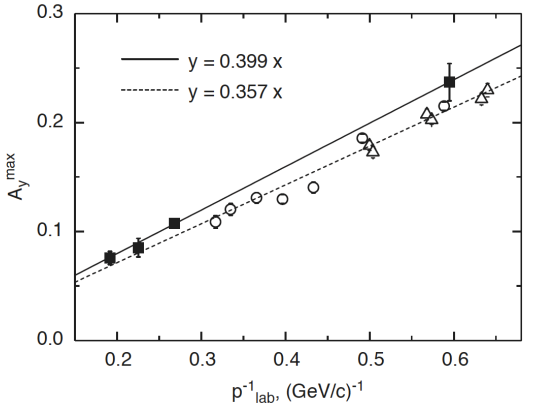

Fig. 5. Momentum dependence of CH_2- and C-data. Solid squares—current data, open circles— Ref. [4], open triangles—Ref. [5]. Solid line—fit of CH_2-data, dashed line—fit of C-data.

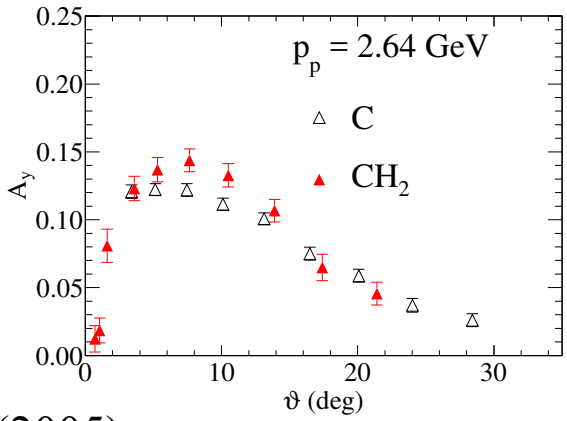

Azhgirey *et al.,* Nucl. Instr. Meth. A, 538, 441 (2005):

- Analyzing power roughly independent of target thickness at 3.8 GeV
- Polarimeter figure-of-merit essentially saturates beyond one nuclear collision length λ_T of CH_2 thickness (at 3.8 GeV proton momentum, anyway) and for transverse momenta $p_T = p_p \sin\vartheta \geq 0.7$ GeV
- CH_2 analyzing power significantly higher than C in the few-GeV momentum range
- Stacking two polarimeters in series, each with approximately one λ_T analyzer thickness, increases FPP FOM by ~1.5

FPP drift chamber design

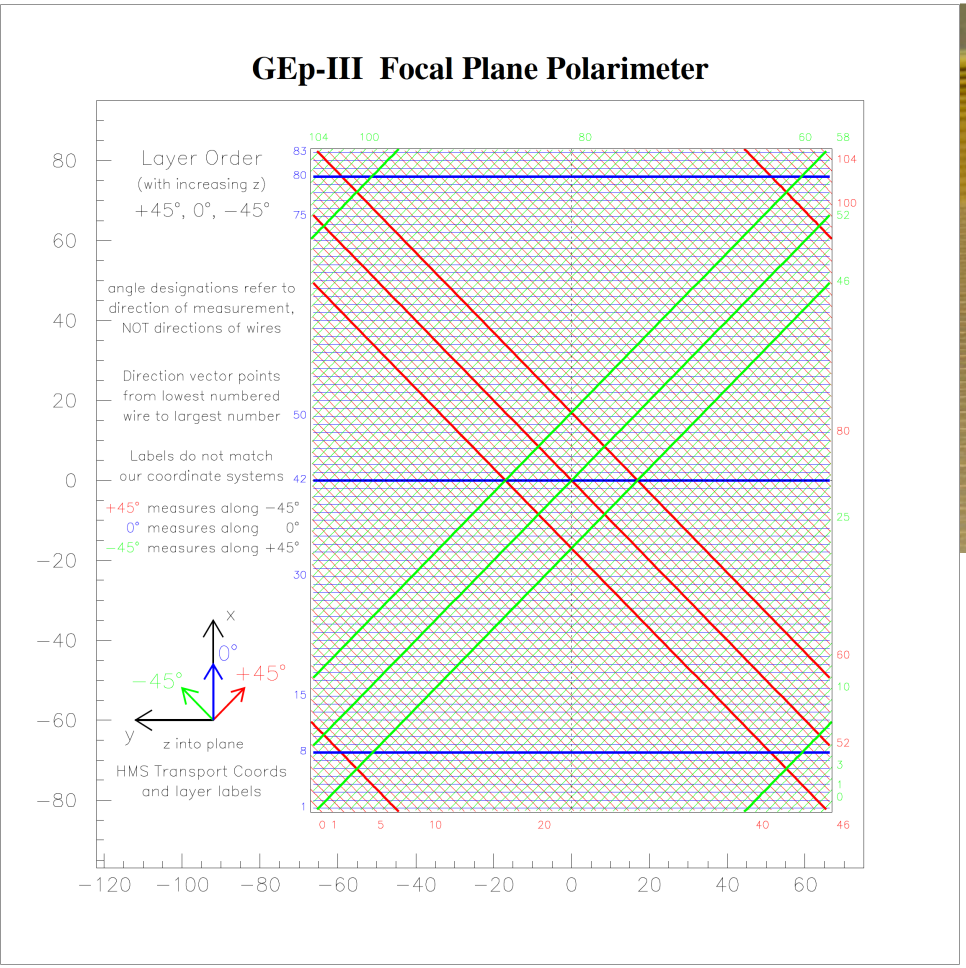

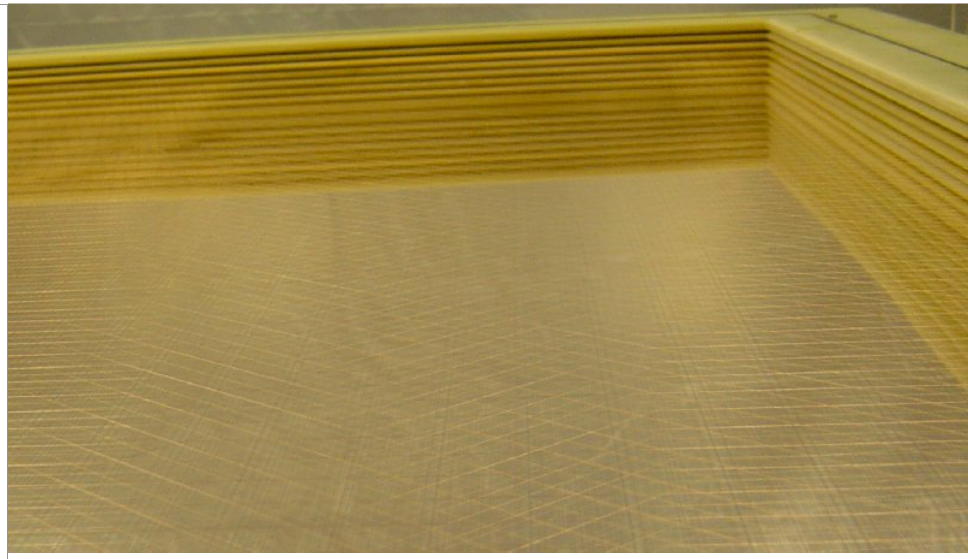

TABLE III. Characteristics of the wires used in the FPP drift chambers. The sense wires are gold-plated tungsten, while the cathode and field wires are made of a beryllium-bronze alloy.

Type	Diameter (μm)	Tension (g)
Sense	30	70
Field	100	150
Cathode	80	120

- Each chamber consists of three planes of sense wires, oriented at $\pm 45°, 90°$ relative to HMS dispersive direction, with 2-cm "pitch"
- Protons tracked after each analyzer by a pair of FPP chambers, ***six planes in total***

- FPP chambers and CH_2 analyzers are on separate support frames, to insure that FPP chambers cannot move upon insertion/retraction of the CH_2 analyzers
- Space in the HMS hut, cost considerations/etc limited the number of wire planes used for FPP tracking system.

FPP performance: coordinate and angular resolution

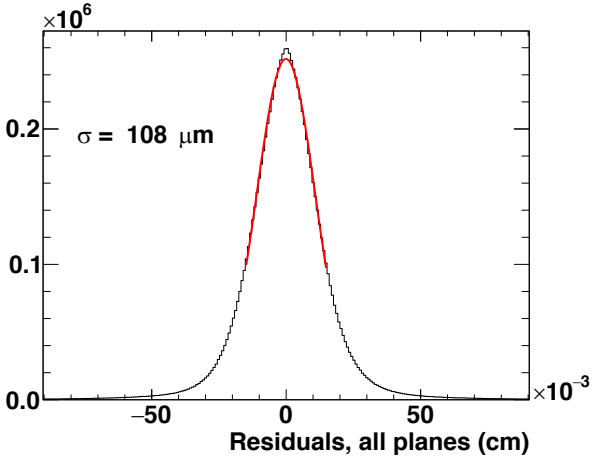

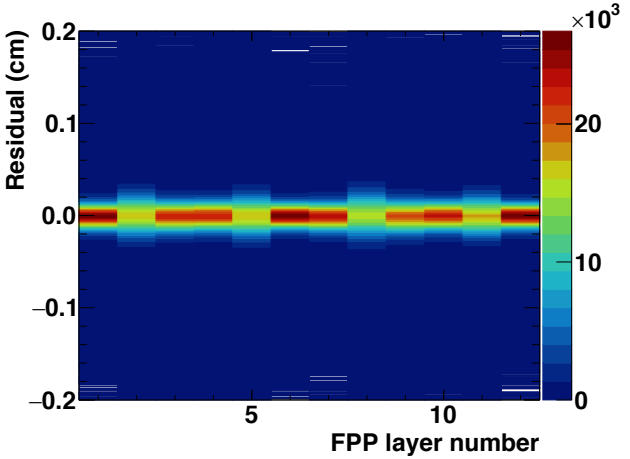

- Width of tracking residuals for straight-through tracks with all six planes firing average about 100 μm for 2.4 GeV electrons, slightly worse for 2.1-5.4 GeV protons.

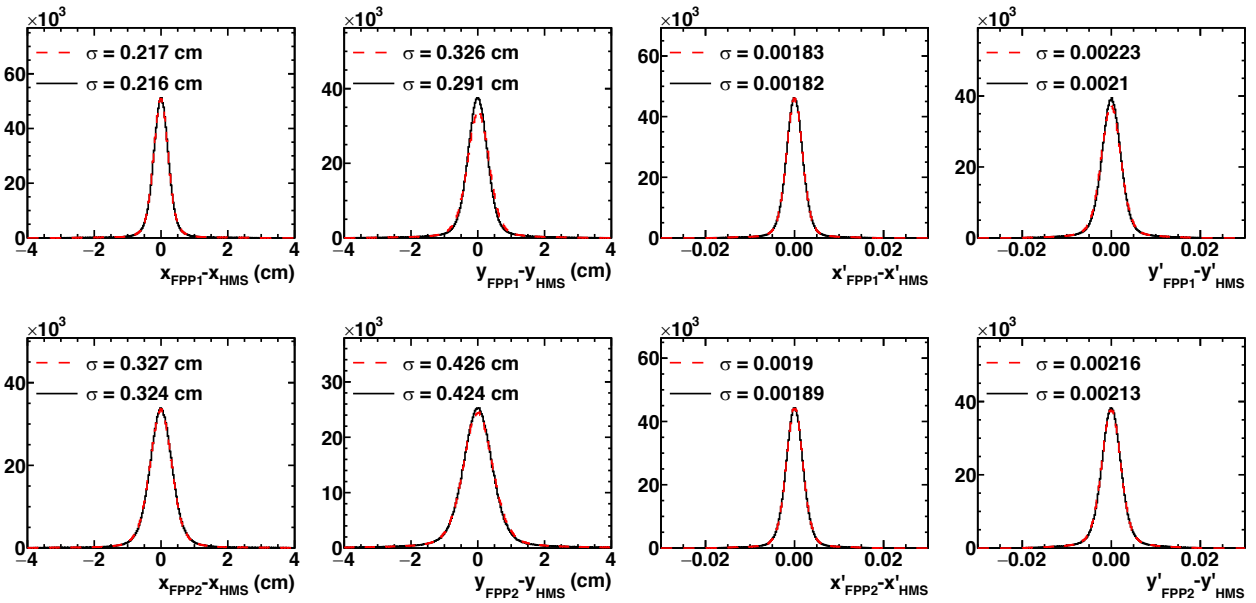

FPP-HMS track parameter differences, **before** (**after**) alignment corrections

- Observed tracking residuals correspond to an intrinsic coordinate resolution of ≈ 270 μm, which is consistent with observed HMS drift chamber resolution (same gas mixture, similar electric field/drift velocity/readout characteristics)
- As measured by track slope differences between FPP/HMS for straight-through tracks, FPP angular resolution is $\sigma_{x'}(\sigma_{y'}) = 1.8\ (2.1)$ mrad. The resolution asymmetry between the "x" and "y" directions results from the orientation/layout of the wire planes.
- The smallest polar scattering angle accepted in the analysis is ~0.5 degrees = 9 mrad (for $Q^2 = 8.5$ GeV^2, $p_p = 5.4$ GeV/c)

FPP event selection criteria

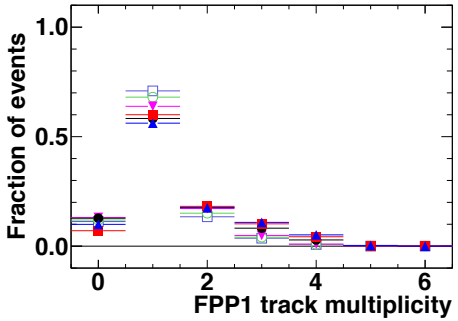

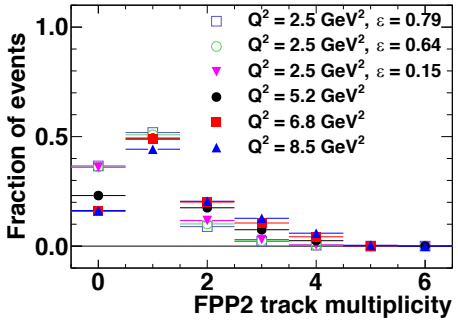

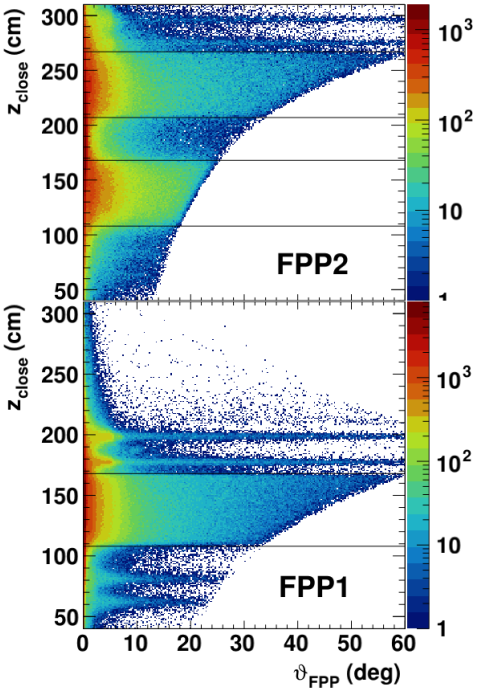

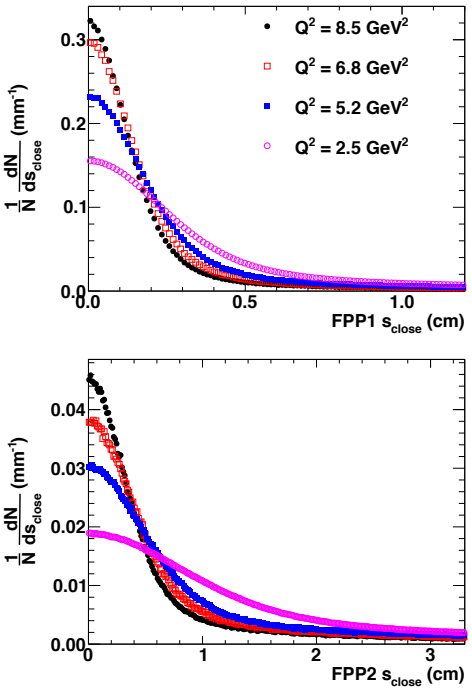

Table 1: FPP event selection criteria as a function of Q^2. Only single-track events passing the "cone test" were included in the analysis. No explicit ϑ cuts were applied. Instead, the ϑ ranges shown are the effective ranges resulting from the p_T cuts. The same criteria were applied to all three ϵ values at $Q^2 = 2.5$ GeV^2. s_{close} and z_{close} are defined, respectively, as the distance of closest approach between the incident and scattered tracks, and the z-coordinate of the point of closest approach between incident and scattered tracks, with $z = 0$ at the HMS focal plane.

Q^2 (GeV^2)	2.5	5.2	6.8	8.5
p_T^{min} (GeV/c)	0.06	0.05	0.05	0.05
p_T^{max} (GeV/c)	1.2	1.5	1.5	1.5
FPP1 ϑ_{min}^{eff}(°)	1.71	0.81	0.65	0.53
FPP1 ϑ_{max}^{eff}(°)	36.7	25.1	19.9	16.3
FPP2 ϑ_{min}^{eff}(°)	1.82	0.84	0.67	0.55
FPP2 ϑ_{max}^{eff}(°)	39.5	26.0	20.4	16.6
FPP1 s_{close}^{max} (cm)	2.2	1.7	1.4	1.2
FPP2 s_{close}^{max} (cm)	6.5	5.1	4.1	3.3
FPP1 z_{close}^{min} (cm)	108	108	108	108
FPP1 z_{close}^{max} (cm)	168	168	168	168
FPP2 z_{close}^{min} (cm)	207	207	207	207
FPP2 z_{close}^{max} (cm)	267	267	267	267

$$p_T \equiv p_p \sin\vartheta$$

- Useful events in the FPP are selected according to the following criteria:
  - Single charged track—multi-track events have low analyzing power, negligible contribution to figure-of-merit
  - Tracks must pass "cone test", requiring the projection of the cone of opening angle ϑ from the point of closest approach between incident and scattered tracks to the rearmost wire plane to be entirely contained within the FPP drift chamber active area (the z-dependent large-ϑ cutoff in the (ϑ, z_{close}) plot is due to the cone test application.
  - Distance of closest approach s_{close} between incident and scattered tracks is required to be less than a reasonable upper limit, chosen to optimize figure-of-merit
  - z_{close}, the "z" coordinate of the point of closest approach between incident and scattered tracks, must lie within the physical extent of the analyzer, with a small additional tolerance to account for detector resolution

FPP polar angle distributions

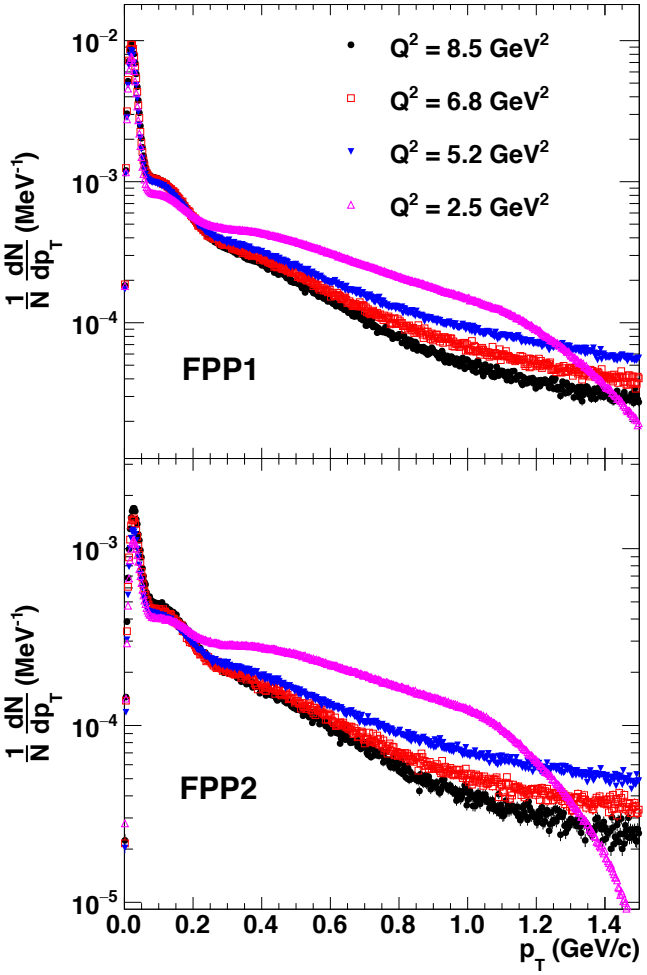

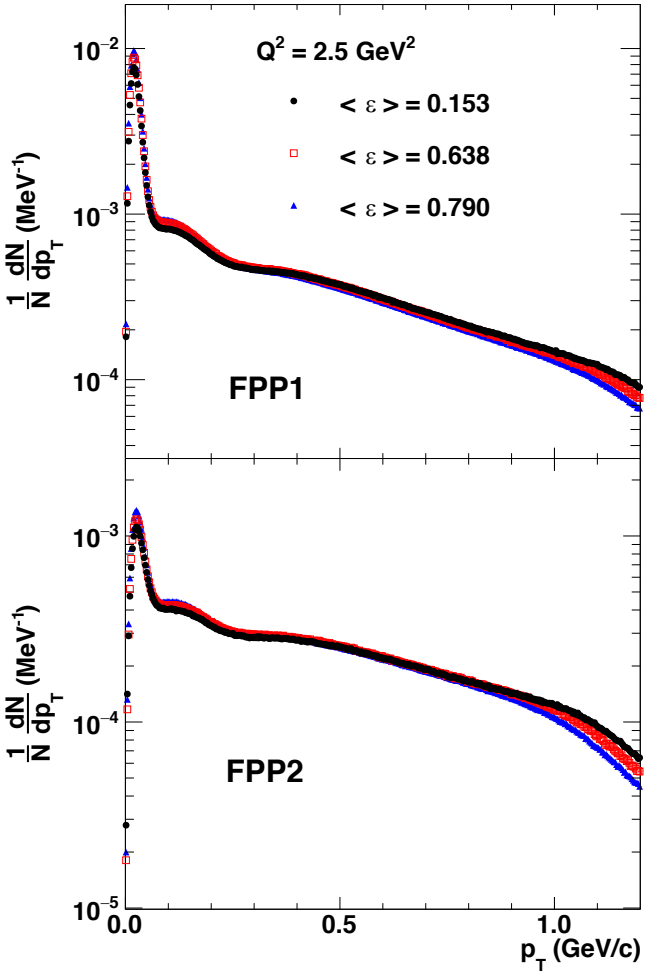

Table 1: FPP event selection criteria as a function of Q^2. Only single-track events passing the "cone test" were included in the analysis. No explicit ϑ cuts were applied. Instead, the ϑ ranges shown are the effective ranges resulting from the p_T cuts. The same criteria were applied to all three ϵ values at $Q^2 = 2.5$ GeV^2. s_{close} and z_{close} are defined, respectively, as the distance of closest approach between the incident and scattered tracks, and the z-coordinate of the point of closest approach between incident and scattered tracks, with $z = 0$ at the HMS focal plane.

Q^2 (GeV^2)	2.5	5.2	6.8	8.5
p_T^{min} (GeV/c)	0.06	0.05	0.05	0.05
p_T^{max} (GeV/c)	1.2	1.5	1.5	1.5
FPP1 ϑ_{min}^{eff}(°)	1.71	0.81	0.65	0.53
FPP1 ϑ_{max}^{eff}(°)	36.7	25.1	19.9	16.3
FPP2 ϑ_{min}^{eff}(°)	1.82	0.84	0.67	0.55
FPP2 ϑ_{max}^{eff}(°)	39.5	26.0	20.4	16.6
FPP1 s_{close}^{max} (cm)	2.2	1.7	1.4	1.2
FPP2 s_{close}^{max} (cm)	6.5	5.1	4.1	3.3
FPP1 z_{close}^{min} (cm)	108	108	108	108
FPP1 z_{close}^{max} (cm)	168	168	168	168
FPP2 z_{close}^{min} (cm)	207	207	207	207
FPP2 z_{close}^{max} (cm)	267	267	267	267

$$p_T \equiv p_p \sin\vartheta$$

- Coulomb scattering dominates for $p_T \leq 0.06$ GeV
- Analyzing power negligible for $p_T \geq 1$ GeV

- Polar scattering angle distribution *approximately* scales with proton momentum, for a given CH_2 thickness.
- At $Q^2 = 2.5\ GeV^2$, the p_T distributions are the same for all three kinematics, at the few-percent level, as expected.

Lesson Learned: Irreducible FPP left-right ambiguity

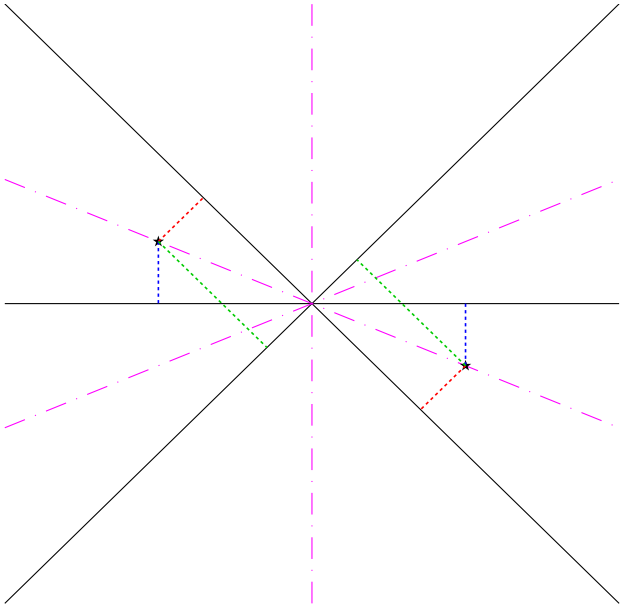

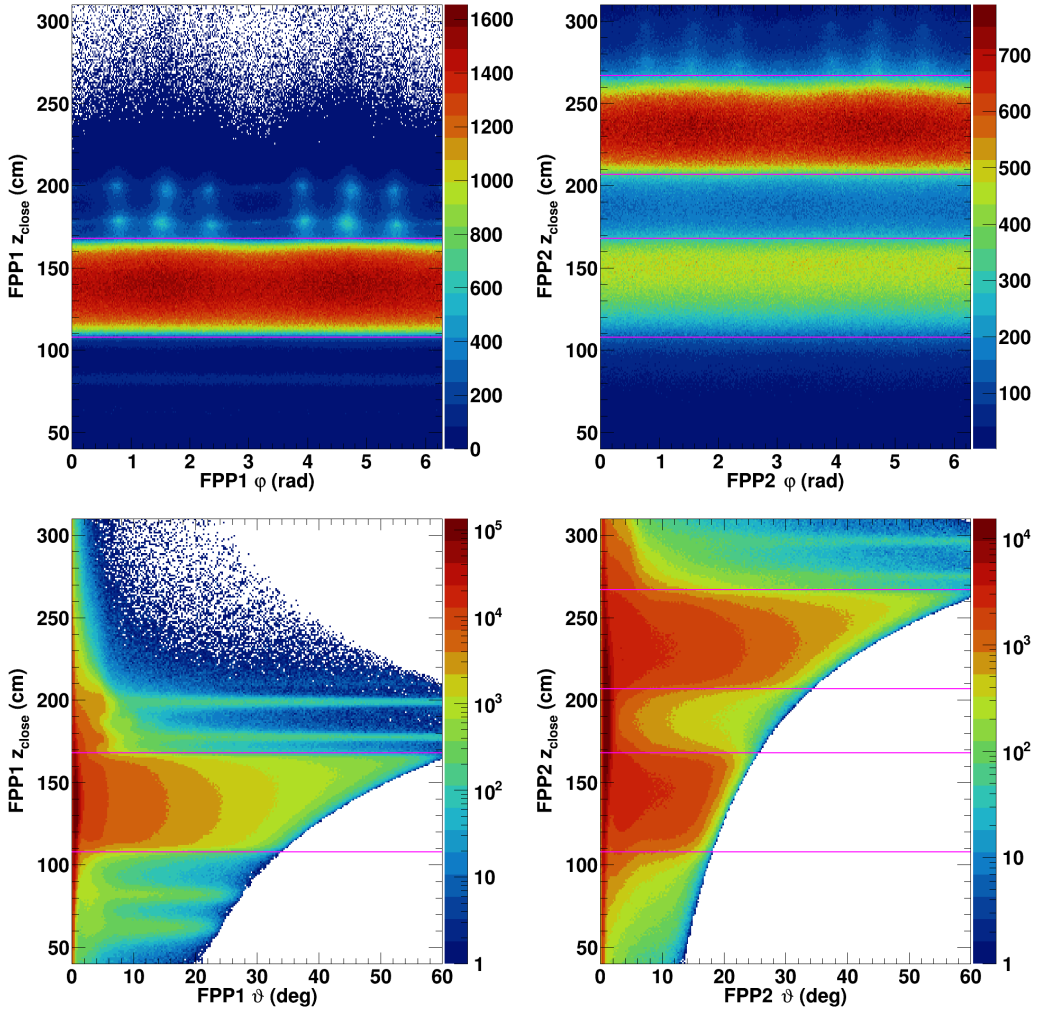

- The symmetry of wire orientations and common intersection point of U, V, X wires at chamber center leads to the existence of two solutions with (nearly) identical χ^2, with hits placed on the opposite side of all three wires firing in a given chamber, for tracks at or near normal incidence.
- Ambiguity cannot be eliminated without introducing scattering-parameter-dependent biases in the pattern recognition and track reconstruction, which is dangerous.
- Ambiguity can be eliminated (for future experiments) by adding more wire planes; e.g., operating in a single-FPP configuration with 12 tracking planes by retracting the second analyzer block, or retaining the double-FPP layout, but slightly reducing the thickness of each analyzer block and adding a third identical chamber to each FPP.

FPP-HMS alignment

With and without straight-throughs

FPP-HMS track correlations, Straight-throughs and protons with CH_2 analyzers in, initial alignment from survey, NO CUTS

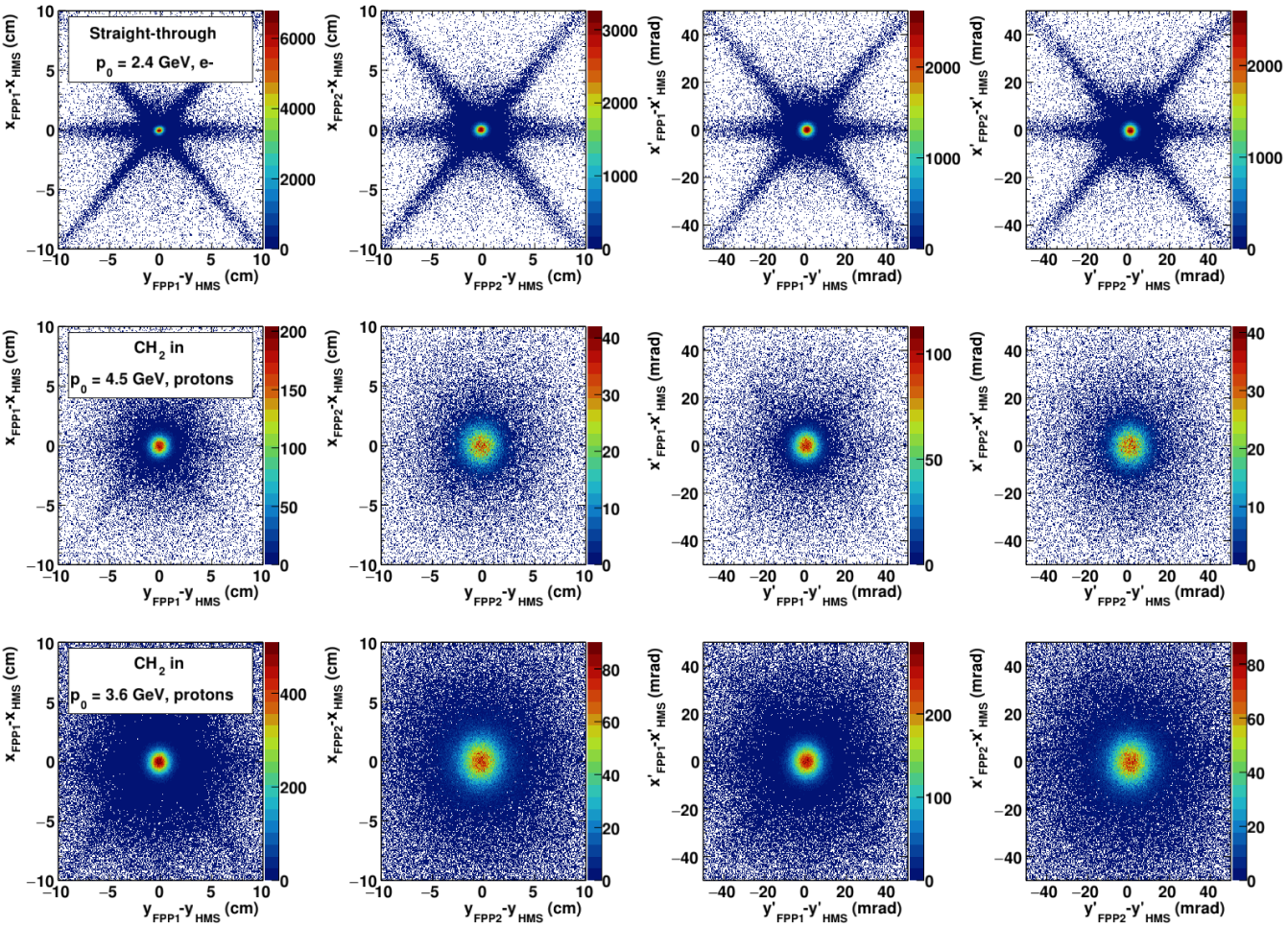

- Note: the "stripes" coinciding with wire orientations, prominent in straight-through data, are pathological "mistracked" events with incorrect left-right assignment.

- Here, we only require a single track in both FPP1 and FPP2, no other cuts on scattering angle, distance-of-closest-approach, etc.

FPP-HMS track correlations, Straight-throughs and protons with CH_2 analyzers in, initial alignment from survey, CUTS

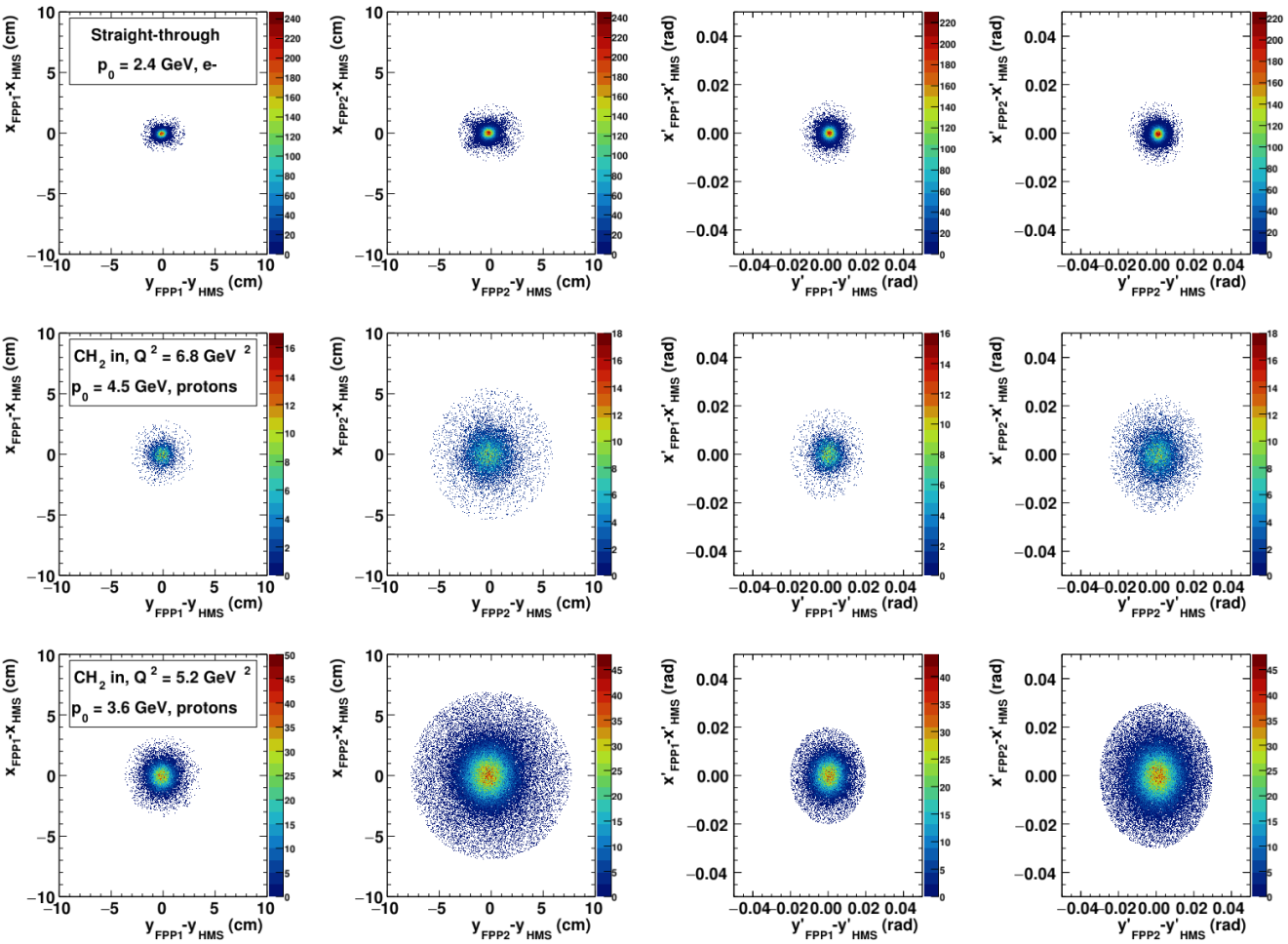

- Note: requirement that both FPP1 and FPP2 tracks pass cuts to include event in alignment analysis is an artifact of the code, which expects straight-through tracks. **With no CH_2, most events pass this criterion.**
- **With CH_2 analyzers in, only ~5% of incident elastic proton events pass these stringent criteria (in the Coulomb-peak of FPP1 and FPP2)**
- With CH_2 analyzers in, we could significantly increase the FPP1 statistics by *not* demanding that events to be included in FPP1 analysis pass FPP2 cuts.
- However, demanding an FPP2 track consistent with no scattering also leads to a "cleaner" event distribution in FPP1, at the price of a significant reduction in statistics.

- Here we require exactly one track in both FPP1 and FPP2, and furthermore, we require that *both* the FPP1 and FPP2 tracks pass a set of scattering angle/closest approach cuts.

One-dimensional projections of track-parameter differences, initial alignment from survey, NO CUTS

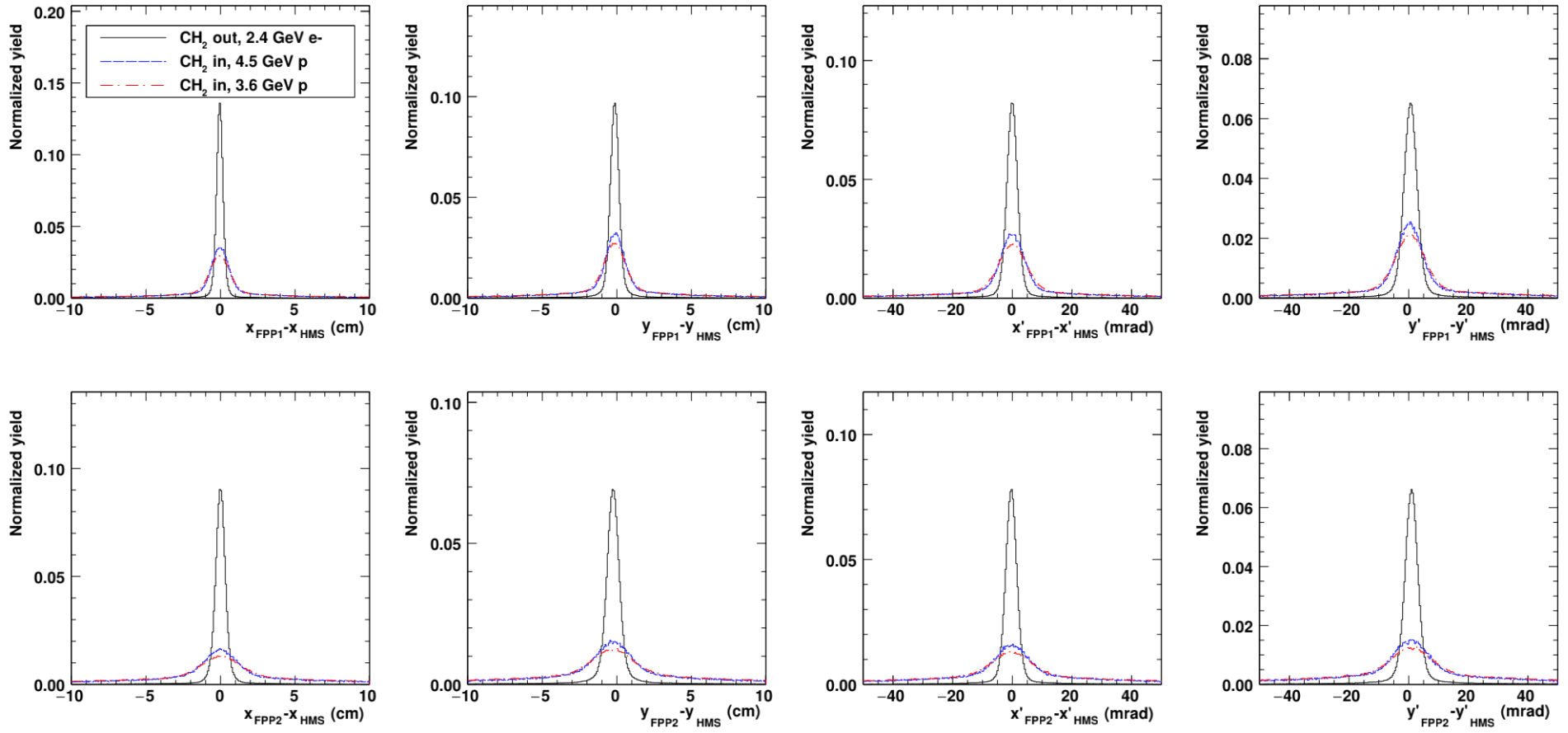

Global Alignment Parameters

Global alignment parameters	x FPP1 (cm),	y FPP1 (cm),	z FPP1 (cm)	FPP1 α_x (mrad)	FPP1 α_y (mrad)	FPP1 α_z (mrad)	x FPP2 (cm),	y FPP2 (cm),	z FPP2 (cm)	FPP2 α_x (mrad)	FPP2 α_y (mrad)	FPP2 α_z (mrad)
FPP survey	-6.5	-1.2	189.1*	0	0	0	-6.4	-1.5	286.6*	0	0	0
CH2 out, 2.4 GeV electrons (Feb. 2008)	-6.44	-1.18	188.2	0.70	0.05	-3.25	-6.29	-1.54	285.8	1.02	0.37	-3.87
CH2 in, 4.5 GeV protons (Q^2 = 6.8 GeV^2, May-June, 2008)	-6.46	-1.19	188.1	0.43	-0.01	-3.02	-6.33	-1.54	285.3	0.95	0.24	-3.99
CH2 in, 3.6 GeV protons (Q^2 = 5.2 GeV^2, Nov. 2007)	-6.45	-1.16	188.0	0.50	-0.08	-2.82	-6.31	-1.51	285.6	0.99	0.38	-3.17

- First step of alignment procedure is to determine the global translational and rotational offsets of each FPP chamber pair that minimize the sum of squared differences between HMS and FPP track parameters (weighted by resolutions). This step converges to an accuracy below the "noise" level in 2-3 iterations
- The optimized chamber center positions, using straight-through or production data, agree with the surveyed positions at the few-hundred-micron level
- The "yaw" (x), "pitch" (y), and "roll" (z) angles agree to within a few tenths of mrad. These angles were not surveyed
- Moreover, these three alignment results come from the beginning (5.2 GeV^2), middle (straight-through electrons) and end (6.8 GeV^2) of GEp-III/2gamma, indicating that the FPP chamber positions and alignment with HMS were stable at this level.
- *--See next slide

Procedure for optimizing z position of chambers

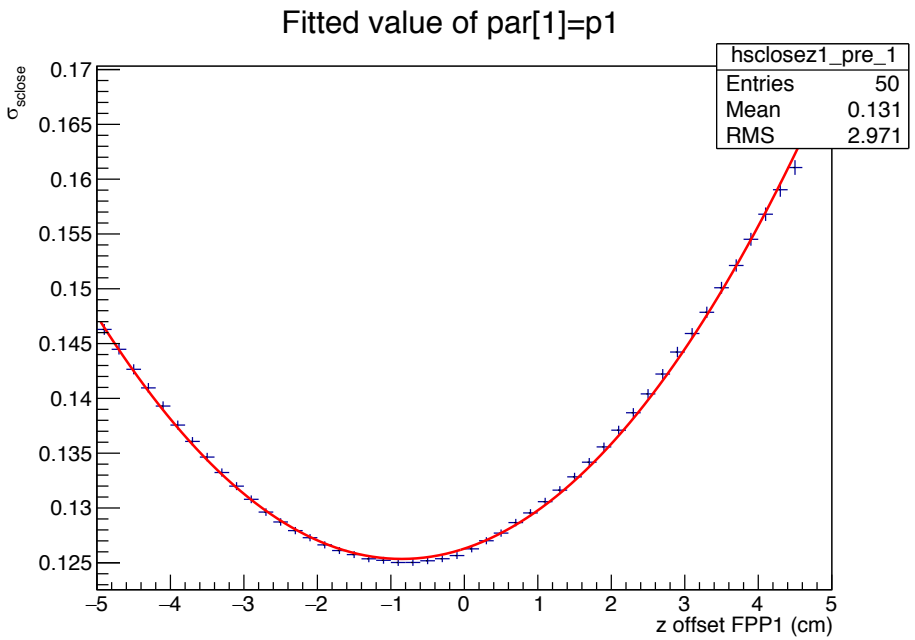

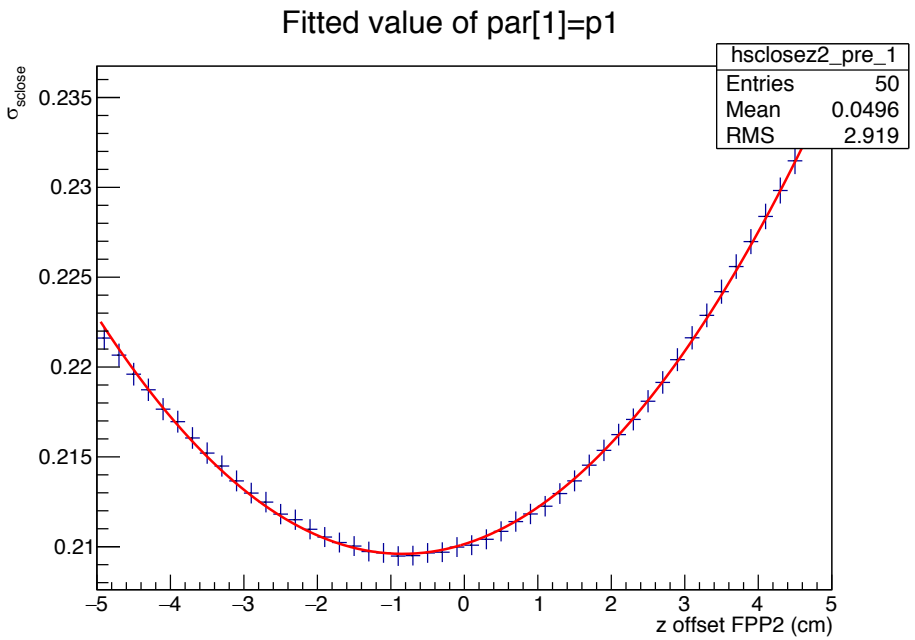

- Straight-through data are not particularly sensitive to a small "z" offset of the chamber positions, because most (straight-through) tracks are nearly perpendicular to the "z" axis of the FPP chambers
- One variable that *is* sensitive to the "z" position is the width of the "sclose" (distance of closest approach) distribution.
- To reveal significant deviations, we have to offset the chamber position by much more than the "allowed" range of ~1-2 mm based on expected accuracy of the surveyed positions
- Data favor an offset of approximately 9-10 mm upstream of the "nominal" position for both chambers: possible that the "nominal" positions were based on a misinterpretation of survey data.
- The uncertainty of the z position determined this way is on the order of 1-2 mm (larger for FPP2), but the consistency between favored FPP1 and FPP2 z offsets suggests that they are real (and they were used in the final PRC analysis)

Residual HMS-FPP track correlations

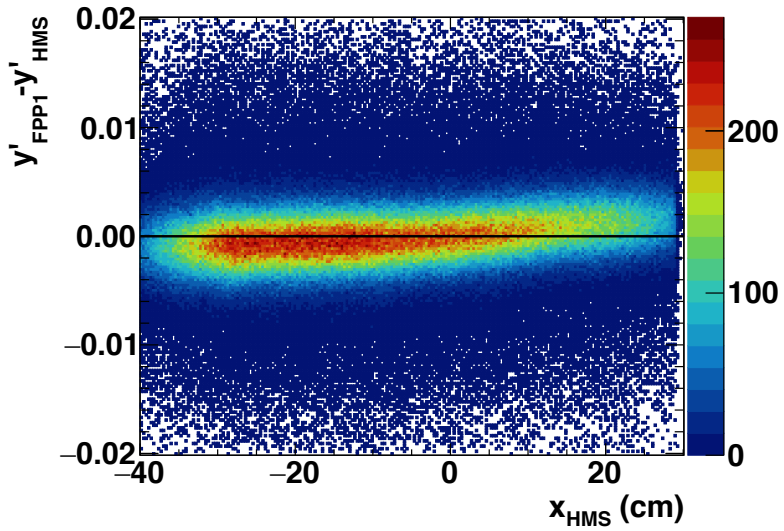

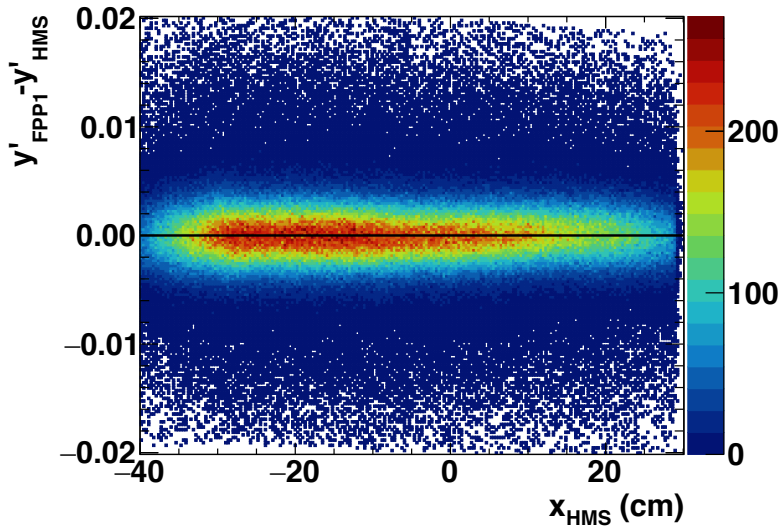

- Even after calibration of internal plane offsets and optimization of global position and orientation parameters, some small residual correlations between FPP-HMS track parameter differences and HMS track parameters remained for straight-through data.
- These kinds of correlations are symptomatic of possible internal misalignments/relative rotations of HMS and/or FPP drift chamber pairs.
- We correct for these in an "ad hoc" fashion by fitting a general 2nd-order expansion of the track differences (in slope and coordinates) as a function of the HMS track parameters, as detailed in http://inspirehep.net/record/1611577
- We then use these parametrized differences to apply (small) corrections to the FPP tracks event-by-event, based on the parameters of the HMS track.

$$\begin{aligned}\Delta u \;=\; & C_0^{(u)} + C_x^{(u)}x + C_y^{(u)}y + C_{x'}^{(u)}x' + C_{y'}^{(u)}y' + \\ & C_{xx}^{(u)}x^2 + C_{xy}^{(u)}xy + C_{xx'}^{(u)}xx' + C_{xy'}^{(u)}xy' + \\ & C_{yy}^{(u)}y^2 + C_{yx'}^{(u)}yx' + C_{yy'}^{(u)}yy' + C_{x'x'}^{(u)}x'^2 + \\ & C_{x'y'}^{(u)}x'y' + C_{y'y'}^{(u)}y'^2, \end{aligned} \tag{6}$$

Results of the "ad hoc" correction (for straight-through data)

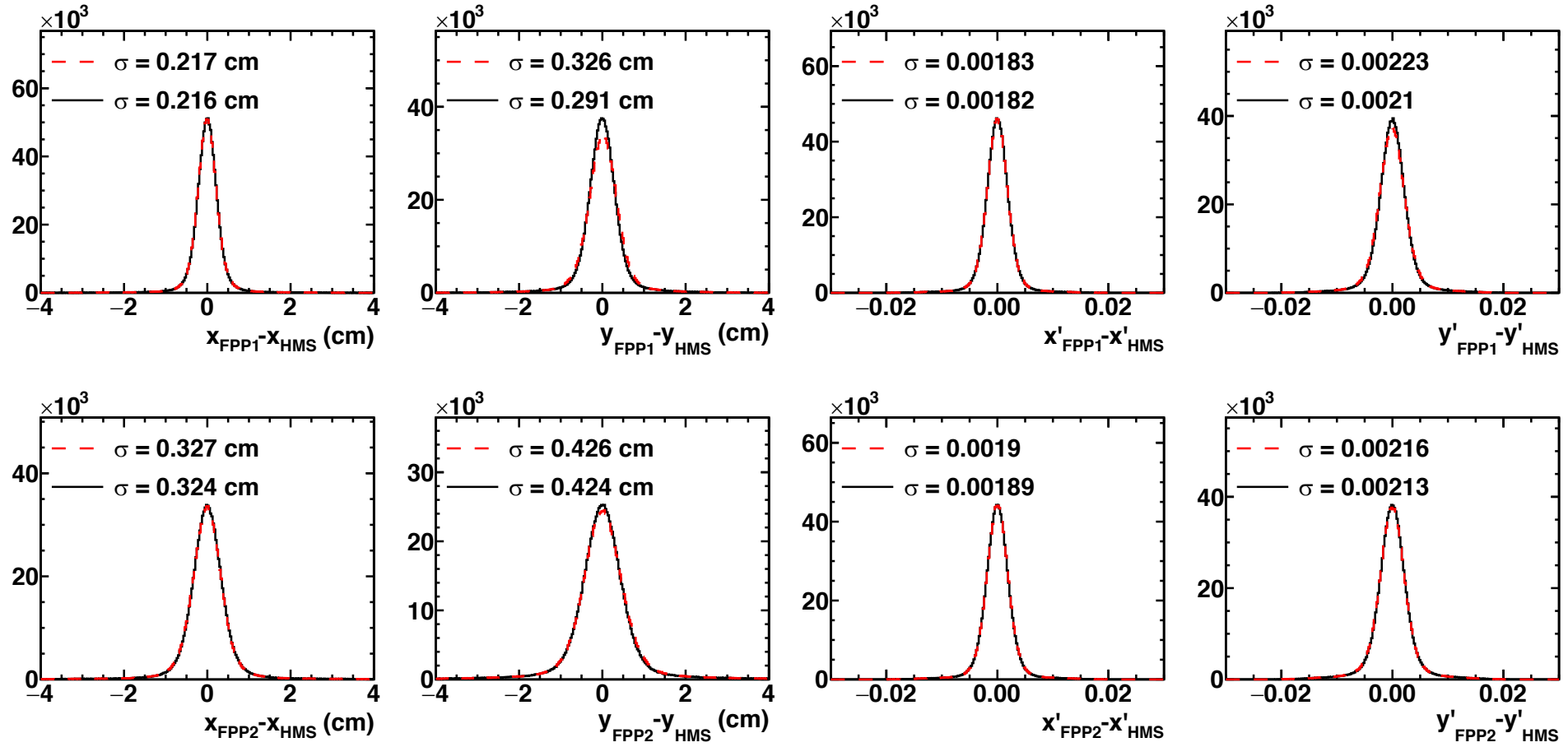

- The correction moderately improves the resolution, particularly for y and y' in FPP1.

FPP alignment Summary and To-Do List

- Preliminary indications are that the *global* alignment parameters of the chambers can be determined with adequate accuracy *without* straight-through data, even at $Q^2 = 5.2$ GeV^2, **HOWEVER:**
  - Without straight-through data, we sacrifice an easy way of independently verifying the quality of the alignment and simplifying a number of other calibration tasks.
  - Without straight-through data, it takes significantly longer to accumulate enough events to calibrate the relative alignment between "front" and "rear" tracking chambers, due to both large-angle scatterings and smearing of the resolution of Coulomb peak events.
- To-do list for FPP-HMS alignment:
  - Reconstruct straight-through tracks with alignment parameters determined from production data for several different kinematics.
  - Check quality of global alignment parameters and *"ad hoc"* quadratic track corrections.
  - Didn't have time to complete analysis/make plots before this meeting, but preliminary results are encouraging.

Final Systematic Uncertainties—Ratio R

Table 3: Systematic uncertainty contributions for $R = -K\frac{P_t}{P_\ell} = \mu_p \frac{G_E^p}{G_M^p}$. The total systematic uncertainty includes the effects of partial correlations among the various systematic contributions, including $\Delta\phi_{tar}$ and Δy_{tar} (correlation coefficient $\rho_{\Delta\phi\Delta y} \approx -0.43$), and $\Delta\theta_{tar}$ and $\Delta\delta$ (correlation coefficient $\rho_{\Delta\theta\Delta\delta} \approx +0.26$). ΔR_{syst}^{total} is the total systematic uncertainty, while ΔR_{syst}^{ptp} is the "point-to-point" systematic uncertainty for $Q^2 = 2.5$ GeV^2 *relative* to the $\epsilon = 0.79$ setting.

Nominal Q^2 (GeV^2)	2.5	2.5	2.5	5.2	6.8	8.5
$\langle\epsilon\rangle$	0.153	0.638	0.790	0.38	0.52	0.24
$\frac{dR}{d\phi_{tar}}\Delta\phi_{tar}$	-3.4×10^{-3}	-2.1×10^{-3}	-2.0×10^{-3}	-4.8×10^{-3}	-5.7×10^{-3}	-0.010
$\frac{dR}{dy_{tar}}\Delta y_{tar}$	-2.0×10^{-3}	-1.2×10^{-3}	-1.2×10^{-3}	-2.9×10^{-3}	-3.9×10^{-3}	-7.7×10^{-3}
$\frac{dR}{d\theta_{tar}}\Delta\theta_{tar}$	-2.2×10^{-3}	-2.5×10^{-3}	-2.5×10^{-3}	1.4×10^{-3}	-5.0×10^{-3}	3.0×10^{-3}
$\frac{dR}{d\delta}\Delta\delta$	5.8×10^{-3}	1.2×10^{-3}	9.0×10^{-4}	1.2×10^{-3}	3.3×10^{-6}	2.5×10^{-4}
$\frac{dR}{d\varphi_{FPP}}\Delta\varphi_{FPP}$	4.1×10^{-3}	2.5×10^{-3}	2.4×10^{-3}	4.6×10^{-4}	-6.0×10^{-3}	-0.017
$\frac{dR}{dE_e}\Delta E_e$	-1.8×10^{-3}	-1.1×10^{-4}	-5.6×10^{-5}	-1.9×10^{-4}	-8.3×10^{-5}	-1.4×10^{-4}
ΔR_{syst}(background)	3.5×10^{-4}	9.6×10^{-5}	9.9×10^{-5}	2.4×10^{-3}	1.6×10^{-3}	0.012
ΔR_{syst}^{total}	7.9×10^{-3}	4.0×10^{-3}	3.9×10^{-3}	5.5×10^{-3}	9.7×10^{-3}	0.024
ΔR_{syst}^{ptp}	4.3×10^{-3}	2.3×10^{-4}	1.1×10^{-4}	N/A	N/A	N/A

- The azimuthal angle reconstruction systematics become *more* sensitive to tracking chamber misalignments at higher energies, due to the useful events for polarimetry being at more forward scattering angles.
- In GEp-III, the systematic uncertainty was obtained by shifting phi by +/- 0.14 mrad/sin(theta) event-by-event. Relative track slope alignment uncertainty between HMS/FPP chambers was estimated at 0.1 mrad based on variations seen among straight-through runs taken under different conditions when reconstructed using the common, final set of alignment parameters.
- This is based on observed rigidity/stability of global FPP alignment at the level of a few hundred microns (see slide 16).
- Rigidity/stability of internal alignment of GEM chamber components and relative alignment of GEM layers within a tracking system (e.g., FT, FPP1, FPP2) should be better yet for higher-Q^2 measurements (and better expected precision).

FPP figure-of-merit considerations

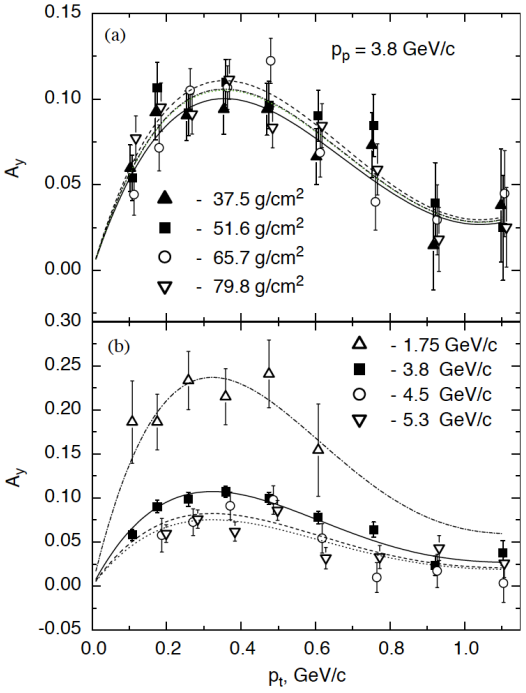

Fig. 4. Analyzing powers as a function of p_t: (a) for different target thicknesses at $p_p = 3.8\,\mathrm{GeV}/c$; (b) for different momenta at $L = 51.6\,\mathrm{g/cm^2}$.

TABLE VI. Experimentally realized effective global FPP efficiencies. "Total elastic events" is the number of events passing the elastic event selection cuts, including the requirement that a definite beam helicity state was recorded for the event. The FPP1 (FPP2) efficiency is the fraction of the total number of elastic events passing all the event selection criteria from Sec. III B 2 for FPP1 (FPP2). Note that the efficiencies quoted here do not include single-track events in FPP2 reconstructed as having scattered in the first analyzer, that failed the event selection criteria for FPP1. These events were included in the GEp-III analysis, but excluded from the GEp-2γ analysis. Note also that the "efficiencies" are not corrected for data runs that were rejected due to data quality issues in either FPP1, FPP2, or both. See text for details.

Q^2 (GeV^2)	$\langle\epsilon\rangle$	Total elastic events ($\times 10^6$)	FPP1 efficiency (%)	FPP2 efficiency (%)	Combined efficiency (%)
2.5	0.153	99.2	20.5	11.5	32.0
2.5	0.638	96.8	23.8	10.6	34.4
2.5	0.790	161.2	26.1	12.8	38.9
5.2	0.382	9.15	16.8	8.6	25.4
6.8	0.519	4.96	17.1	8.0	25.1
8.5	0.243	5.01	15.0	7.0	22.0

- The statement that FPP figure of merit saturates at 1 nuclear collision length of CH_2 thickness is largely based on measurements at a single proton momentum of 3.8 GeV (with large uncertainties).
- Hall C experience shows that the combined efficiency of a double-FPP of constant CH_2 thickness also decreases with momentum (due to decreasing scattering probability in the useful p_T range). It is likely that as the proton momentum increases, the optimal thickness of CH_2 increases as well.

- **Complication:** in SBS, the proton arm trigger is based on HCAL, which is located *behind* both CH_2 analyzers.
  - In all previous PT measurements in Halls A/C, the trigger was based on thin scintillators located *in front of* the FPP chambers, meaning that there was no trigger bias in the angular distribution of secondary scatterings.
- This means that a significant fraction (~30%, next slides) of events that undergo useful scatterings in the *first* analyzer are lost due to subsequent interactions in the second analyzer, which scatter the proton out of the useful acceptance or otherwise absorb enough of its energy to prevent trigger formation.
- It also potentially complicates the analysis, by possibly introducing instrumental asymmetry due to phi-dependent efficiency variations.
- There is reason to expect that triggering only on high-energy protons will actually *increase* the effective analyzing power of the sample of events used for polarimetry; however, this is unproven, and we probably shouldn't count on this to meaningfully increase FOM.

Reminder: GEP Trigger analysis with "L2" logic

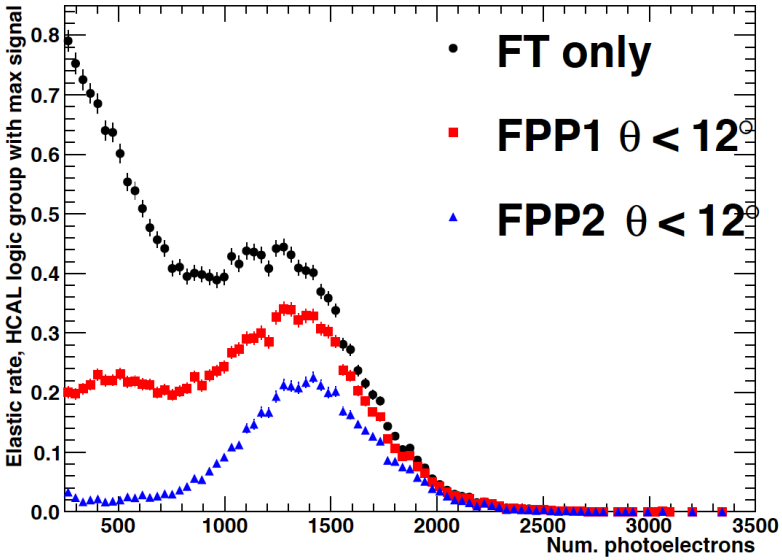

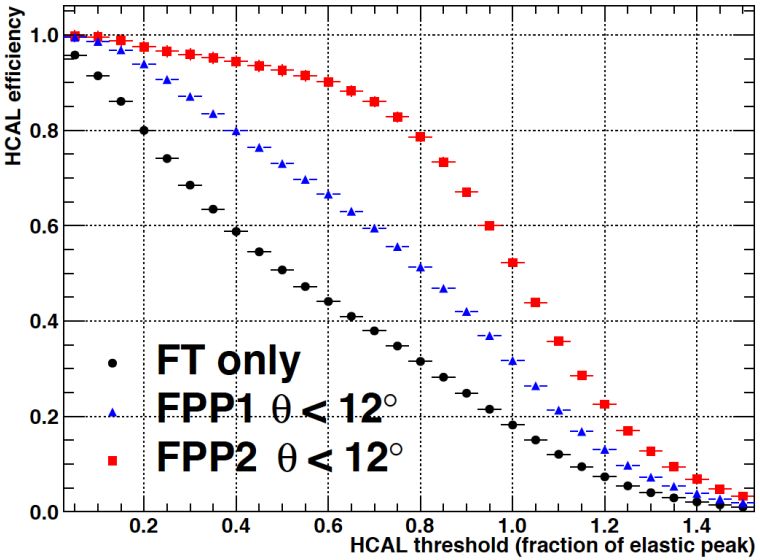

- Signal in HCAL logic group with max signal for elastic ep events, with different cuts on FPP event topology (top left)
- Top right: HCAL trigger efficiency vs. threshold for different event topologies
- Bottom right: Dependence of efficiency on FPP scattering angle in FPP1 (2)

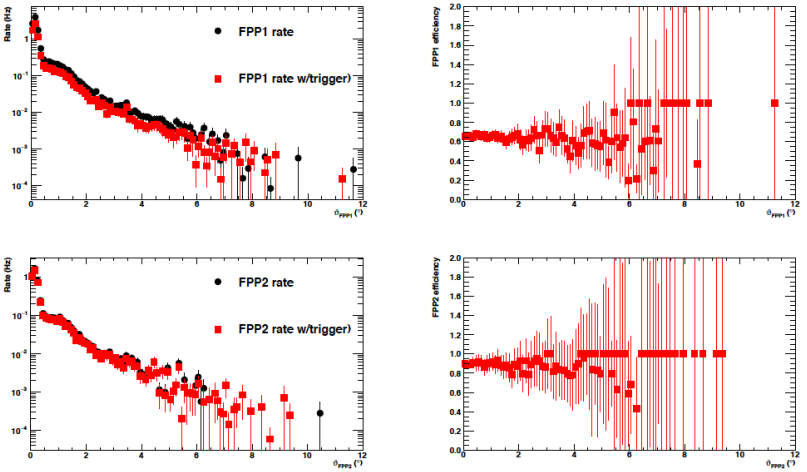

Correlated ECAL-HCAL trigger efficiency

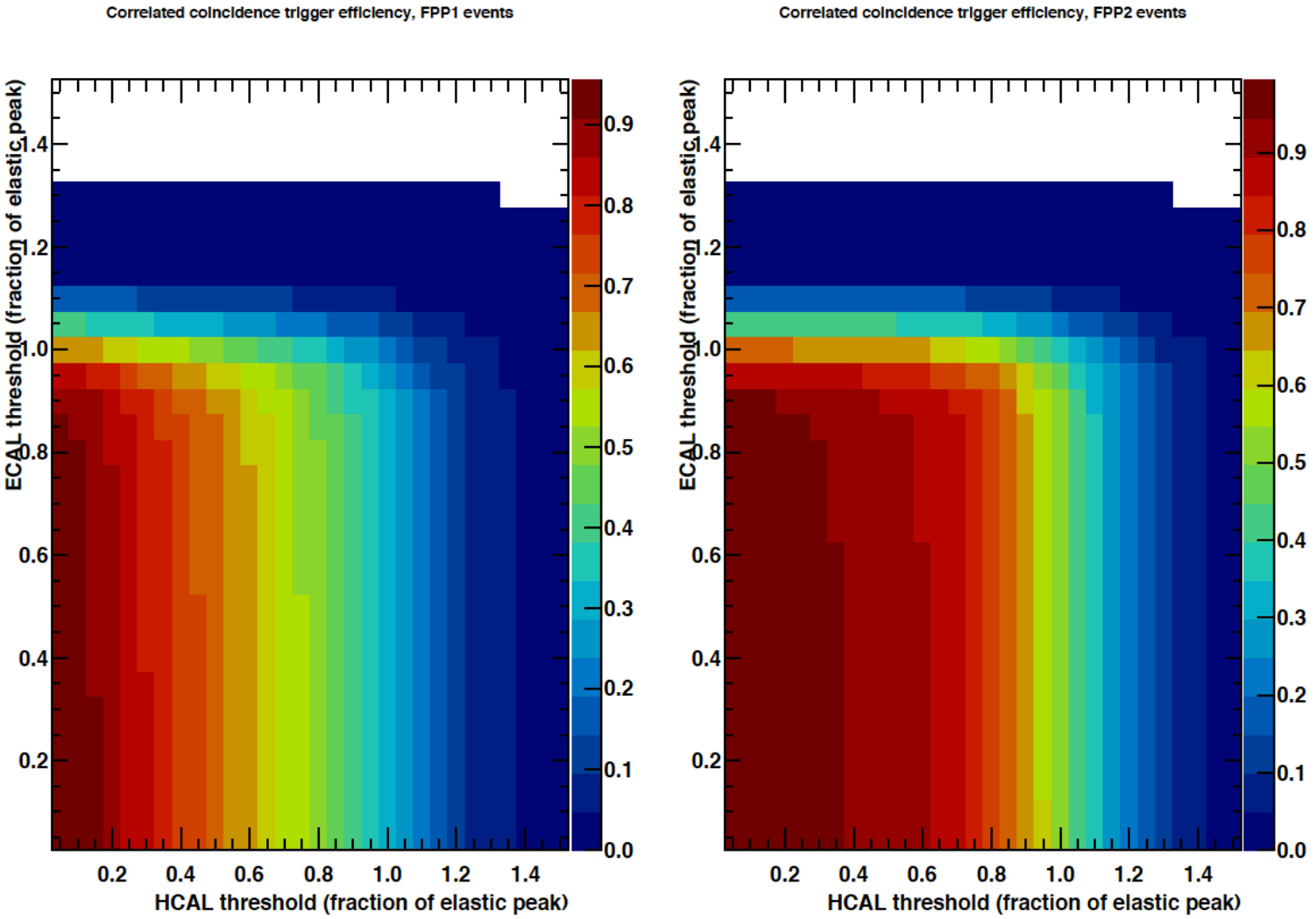

For events with a "good" scattering in FPP1 (left) and events with a "good" scattering in FPP2 (right).

ECAL-HCAL Kinematic Correlations in "Level 2" Coincidence Trigger

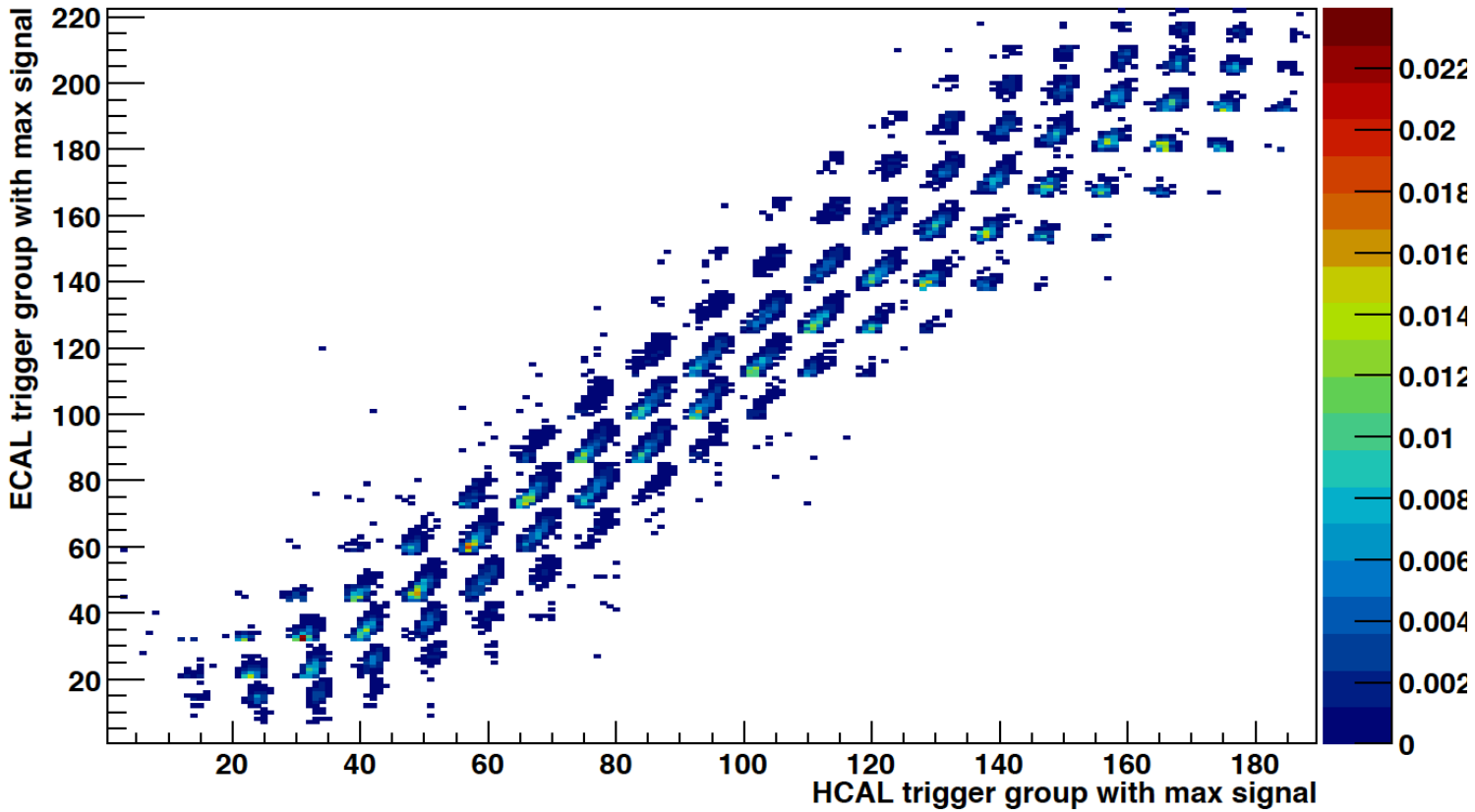

Implement ep angular correlations in the coincidence trigger, by listing for each HCAL trigger sum all ECAL trigger sums exceeding 0.1% of the total event rate

New: GEP Trigger rates with "L2" HCAL logic

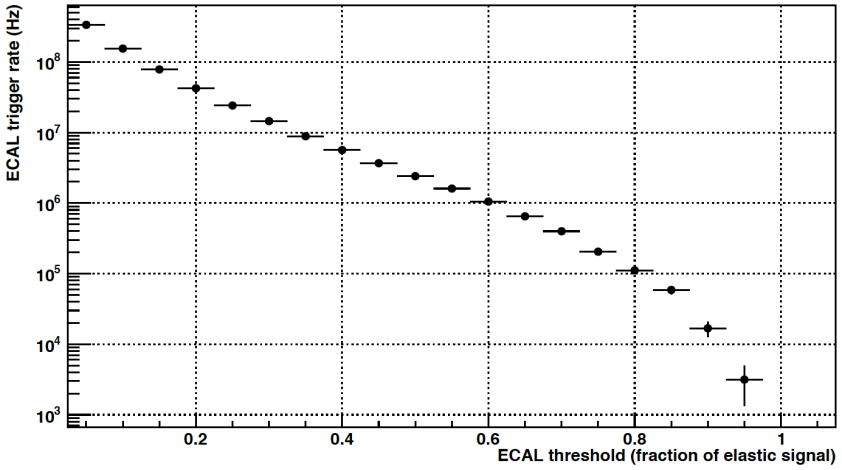

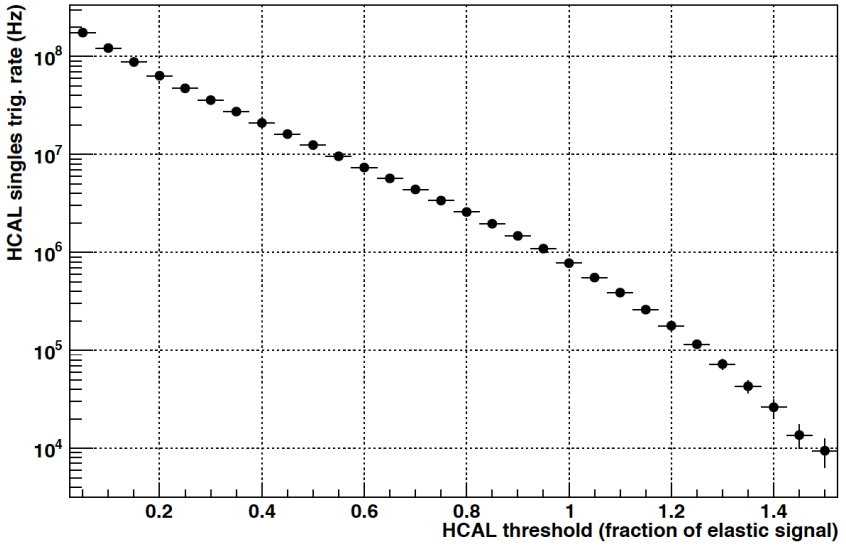

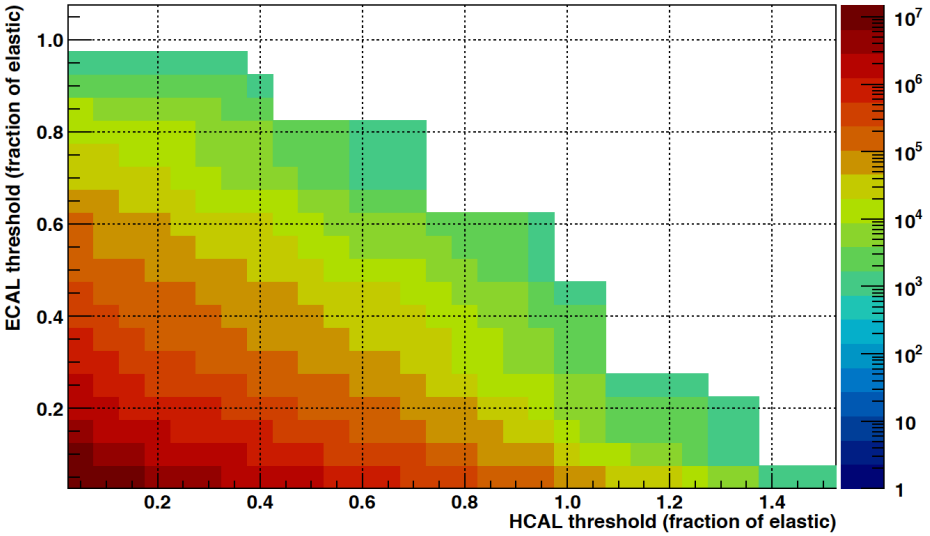

- Top left: ECAL trigger rate vs threshold
- Top right: HCAL L2 trigger rate vs threshold (based on global OR of all possible 4x4 sums of HCAL signals)
- Bottom left: real coincidence rate (PYTHIA6 events) vs ECAL/HCAL thresholds.
- TO DO: analysis of accidentals (not trivial for correlated coincidence trigger with many overlapping logic combinations)

Note on elastic event rates and FOM

- Total FT ($10.5 < Q^2 < 14$ GeV^2): ~25 Hz
- Total FPP1 ($10.5 < Q^2 < 14$ GeV^2): 12 Hz (including small-angle Coulomb)
- Total FPP2 ($10.5 < Q^2 < 14$ GeV^2): 5 Hz (including Coulomb)
- If HCAL trigger efficiency for FPP1 events is 70% and FPP2 efficiency is 90%, the total "good event" rate is:
  - Rate = 0.7*12 Hz + 0.9 * 5 Hz = 12.9 Hz
- Suppose instead that we only used one FPP, with an efficiency of 90%. Then we would have:
  - Rate = 0.9*12 Hz = 10.8 Hz
- Therefore, efficiency gain from using double-FPP in SBS is about 1.2, not ~1.5 as in GEp-III.
- I have assumed that the angular distribution and the average analyzing power are the same for both FPPs

FPP1 and FPP2 angular distributions

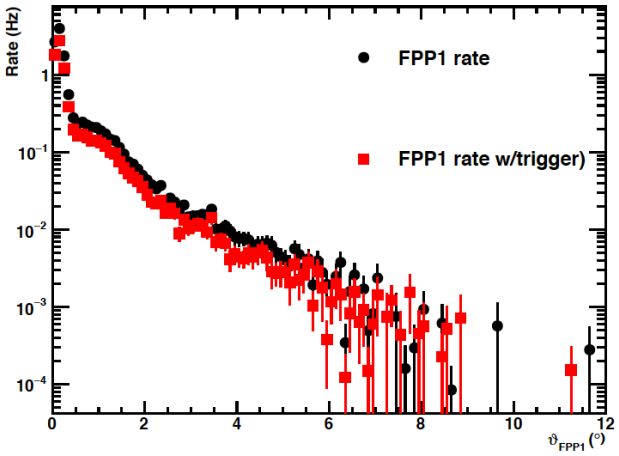

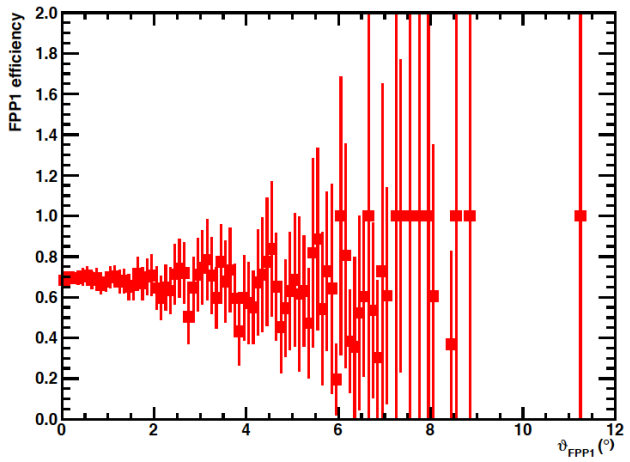

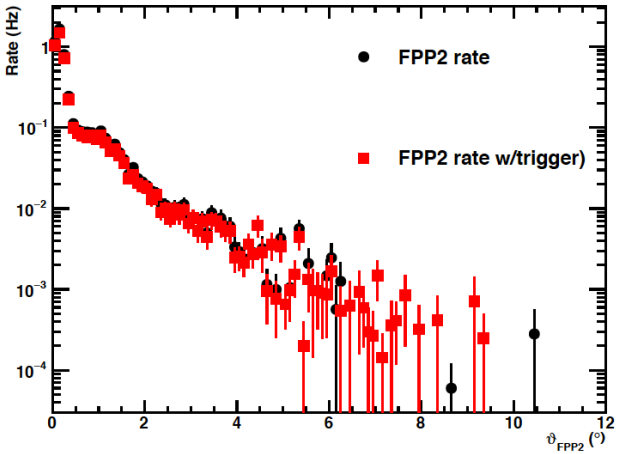

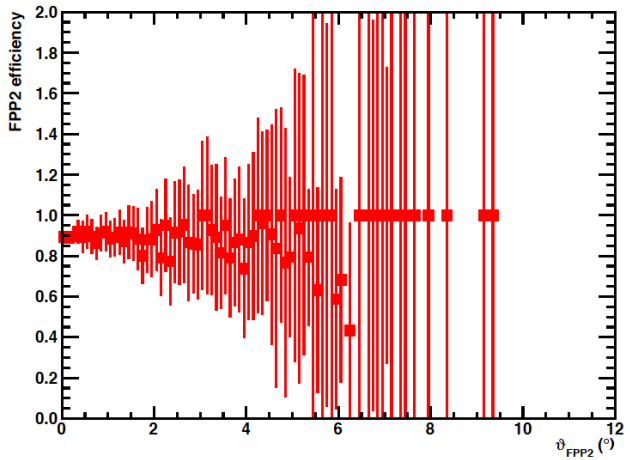

Note: HCAL efficiencies roughly independent of scattering angle for "good" FPP1 and FPP2 events

FPP FOM—Should we revisit CH_2 thickness/layout?

- The fact of the trigger being located behind the polarimeter raises important questions as to whether the layout of tracking detectors and CH_2 analyzers as proposed/designed is optimal from a FOM perspective.
- If the support frame has to be redesigned anyway, should we look at this issue in MC too?
  - I suspect, given the trigger scheme, that asymmetric thicknesses could improve the overall FOM, even without changing the total thickness.
  - Plan to look at 60/40 and 70/30 ratios of FPP1/FPP2 CH_2 thickness in more detail than crude estimates shown above

FT stability/rigidity implications for optics/spin transport

SBS and BigBite Optics/Resolution from g4sbs—Old results

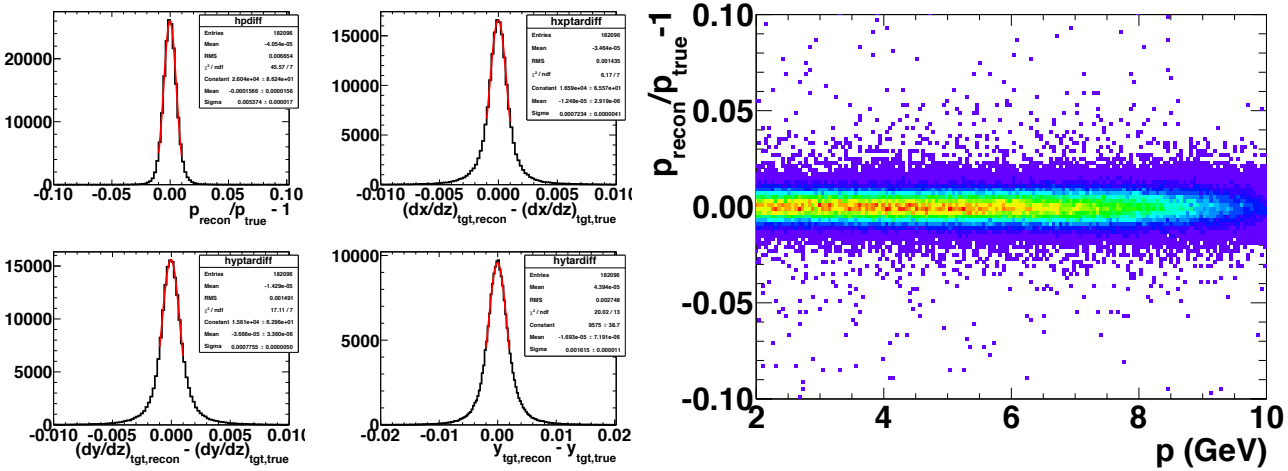

SBS angle, vertex and momentum resolution for 1.4-Tesla uniform field, $\sigma_p/p \sim 0.5\%$ (average for 2-10 GeV pions)

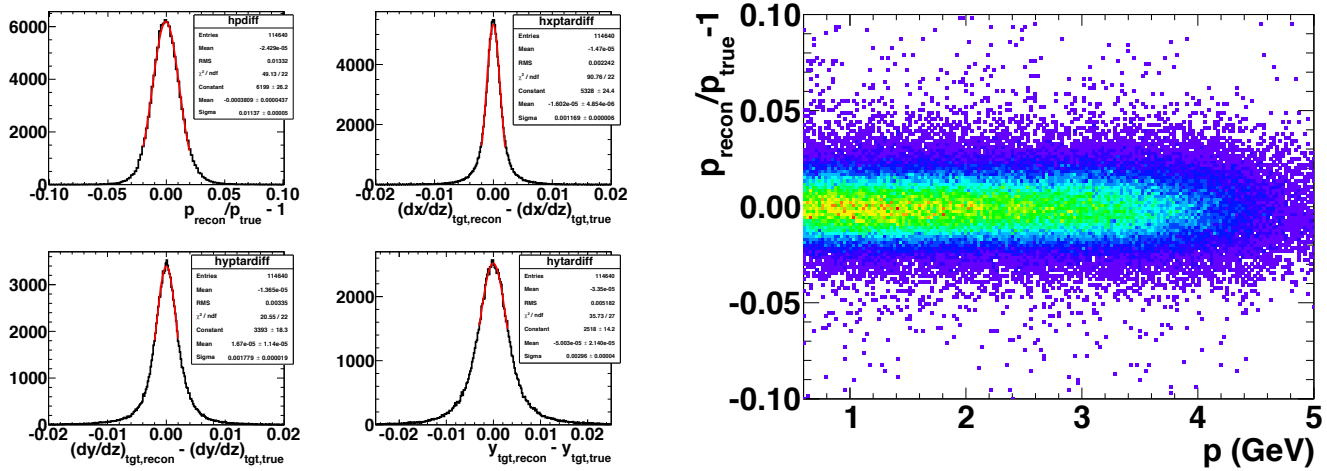

BigBite angle, vertex and momentum resolution for "map_696A.dat", $\sigma_p/p \sim 1.1\%$

Optics and Spin Transport Studies for GEP, $Q^2 = 12$ GeV^2

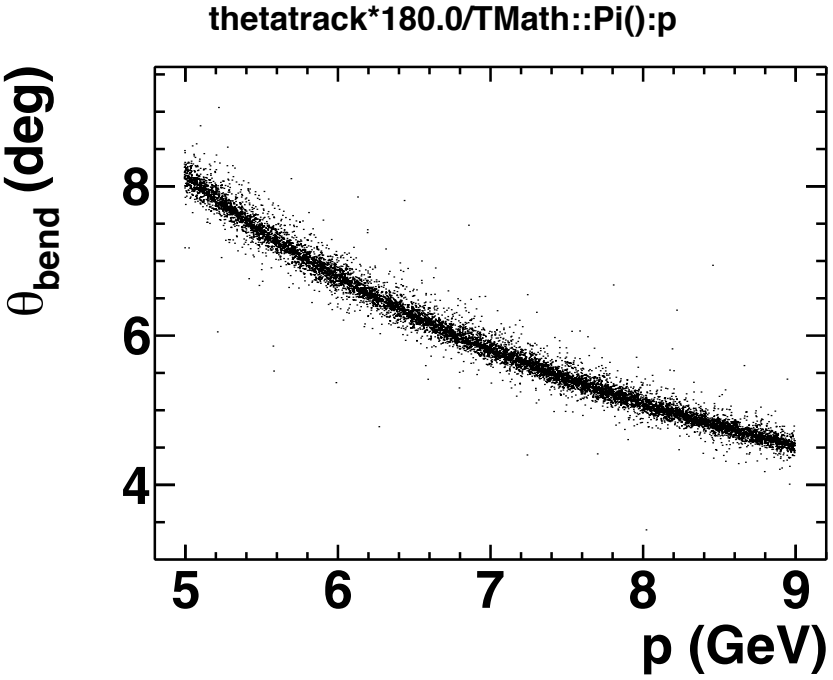

Track vertical bend angle vs. momentum

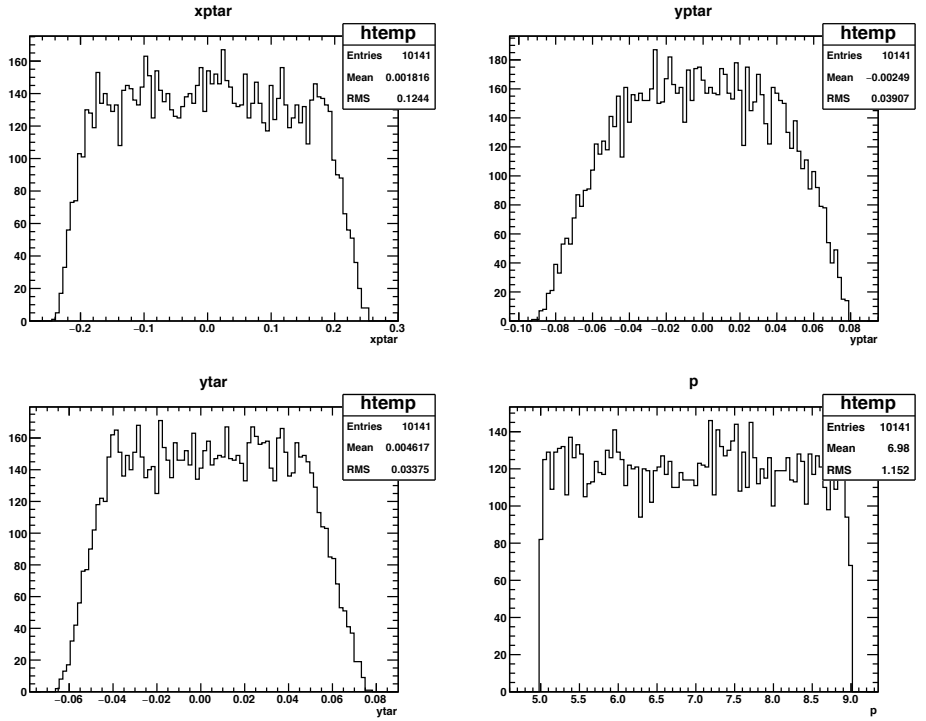

SBS angular and vertex acceptance for GEP highest Q^2

- GEANT4 simulation for optics and spin transport:
  - Use "particle gun" generator with limits chosen wide enough to populate full acceptance of SBS (use 40 cm target)
  - Proton momenta generated in the range of 5-9 GeV (corresponding to highest Q^2 of GEP)
  - Generate 10,000 protons in three different starting spin orientations in the fixed TRANSPORT coordinate system:
    - Pure "X" (vertically down)
    - Pure "Y" (horizontal, toward small angle)
    - Pure "Z" (along SBS central ray)
  - Fit reconstruction coefficients and spin transport matrix elements

SBS optics fitting from GEANT4

- SBS angle, vertex and momentum resolution for 5-9 GeV protons
- sigma(xptar) ~ 0.3 mrad
- sigma(yptar) ~ 0.6 mrad
- sigma(ytar) ~ 1.5 mm
- sigma(p)/p ~ 0.66%
- Improvement of the fit not significant beyond about 4th-order expansion of reconstruction coefficients

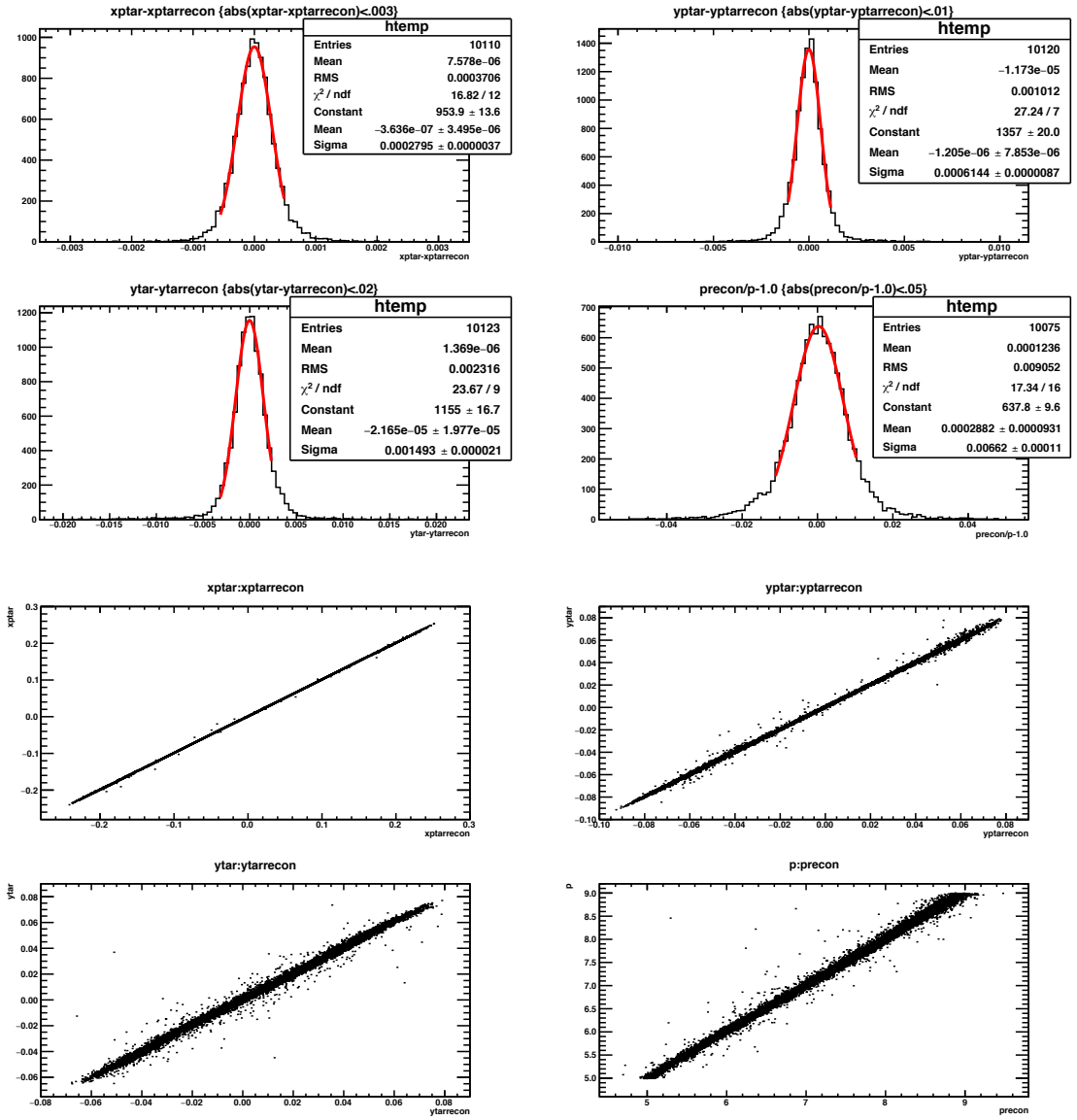

Spin transport properties of SBS in GEP

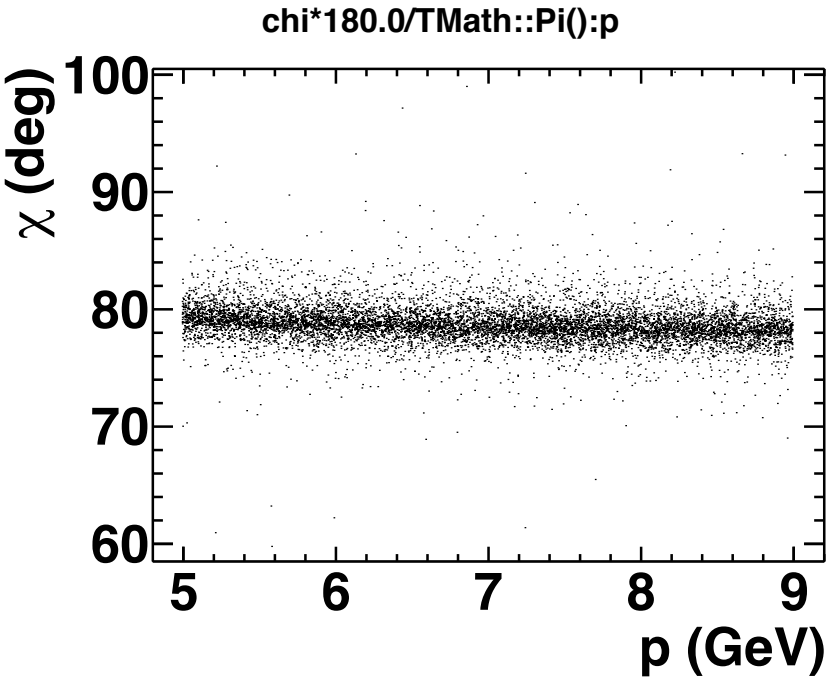

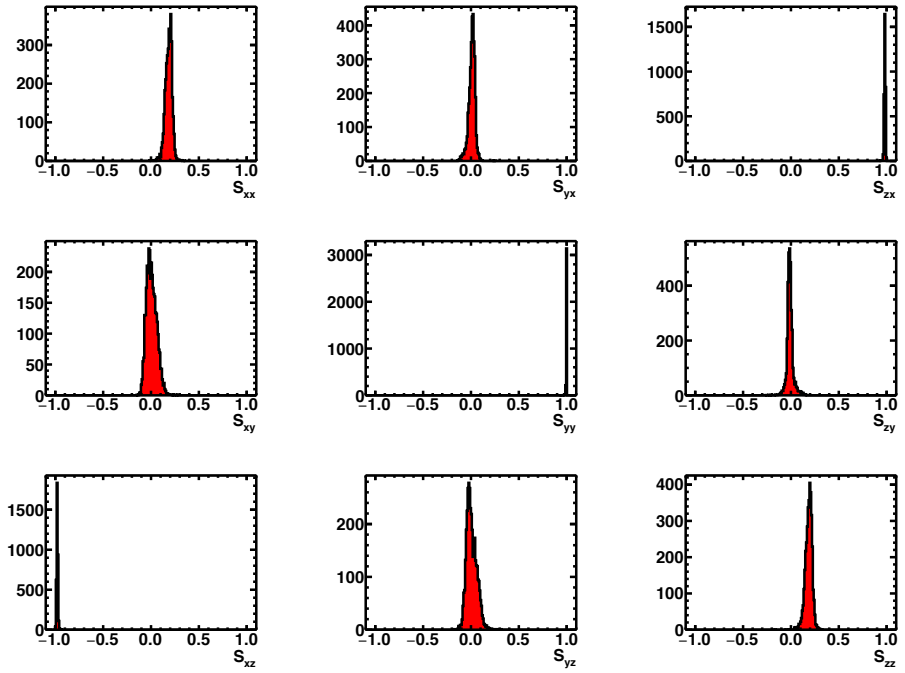

$$\frac{d\mathbf{S}}{dt} = \frac{e}{m\gamma}\mathbf{S} \times \left[\frac{g}{2}\mathbf{B}_{\parallel} + \left(1 + \gamma\left(\frac{g}{2} - 1\right)\right)\mathbf{B}_{\perp}\right]$$

BMT equation for protons

- Spin precession in a magnetic field for is governed by the BMT equation
- For an almost pure dipole field, as in SBS, the proton spin precesses relative to its trajectory by an angle: $\chi = \gamma\kappa_p\theta_{bend}$

- Precession angle is almost constant within useful acceptance of SBS for elastic ep events (cancellation between momentum dependence of gamma and thetabend)

Differences between dipole and full calculation

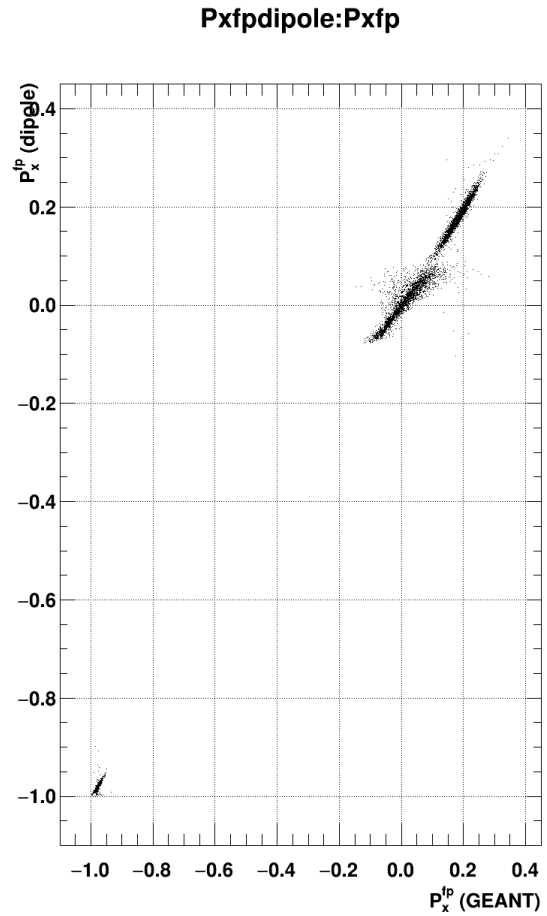

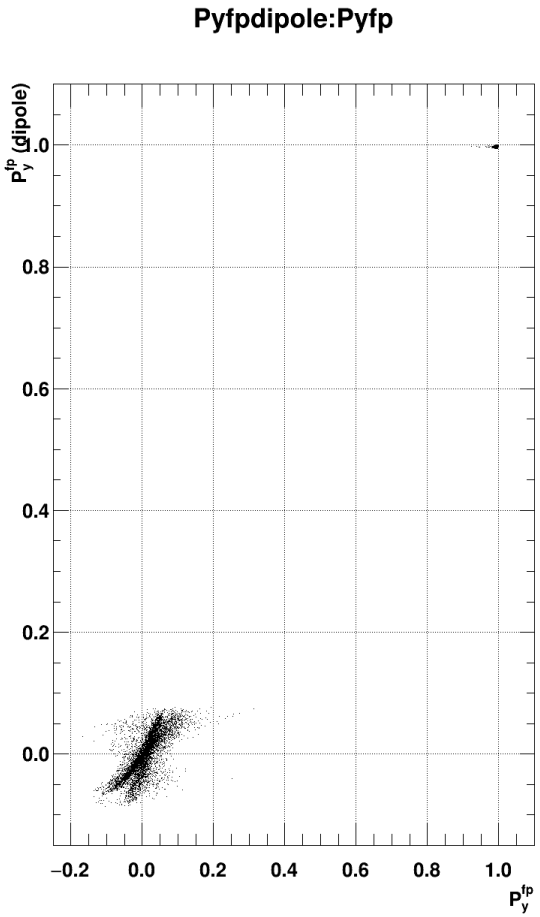

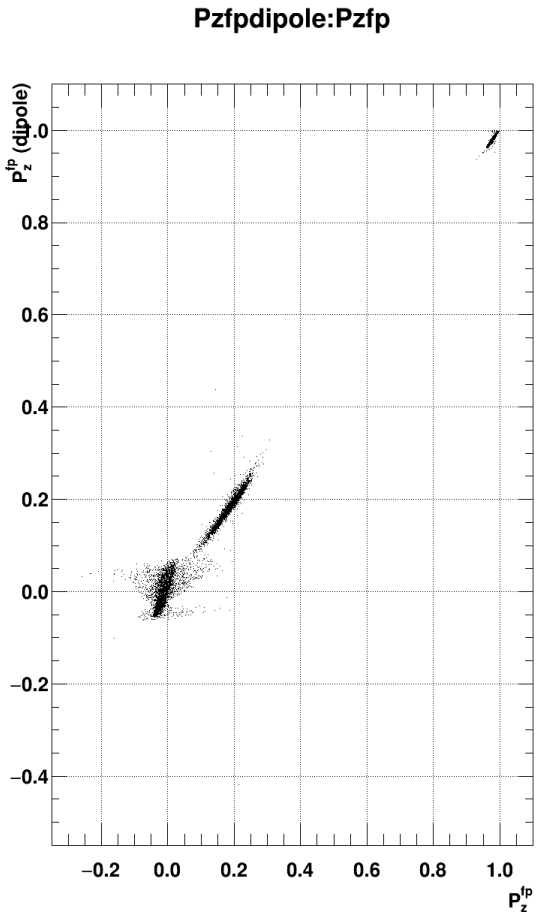

- In dipole approximation, the spin component parallel to the field (Py) does not precess;
- Since SBS is non-focusing, the trajectory bend angle in the non-dispersive plane is close to zero for most trajectories
- Nevertheless, a small precession in the non-dispersive plane occurs for non-central trajectories
- This precession mixes P_T and P_L in extraction of GEp—important systematic uncertainty

Non-dispersive precession

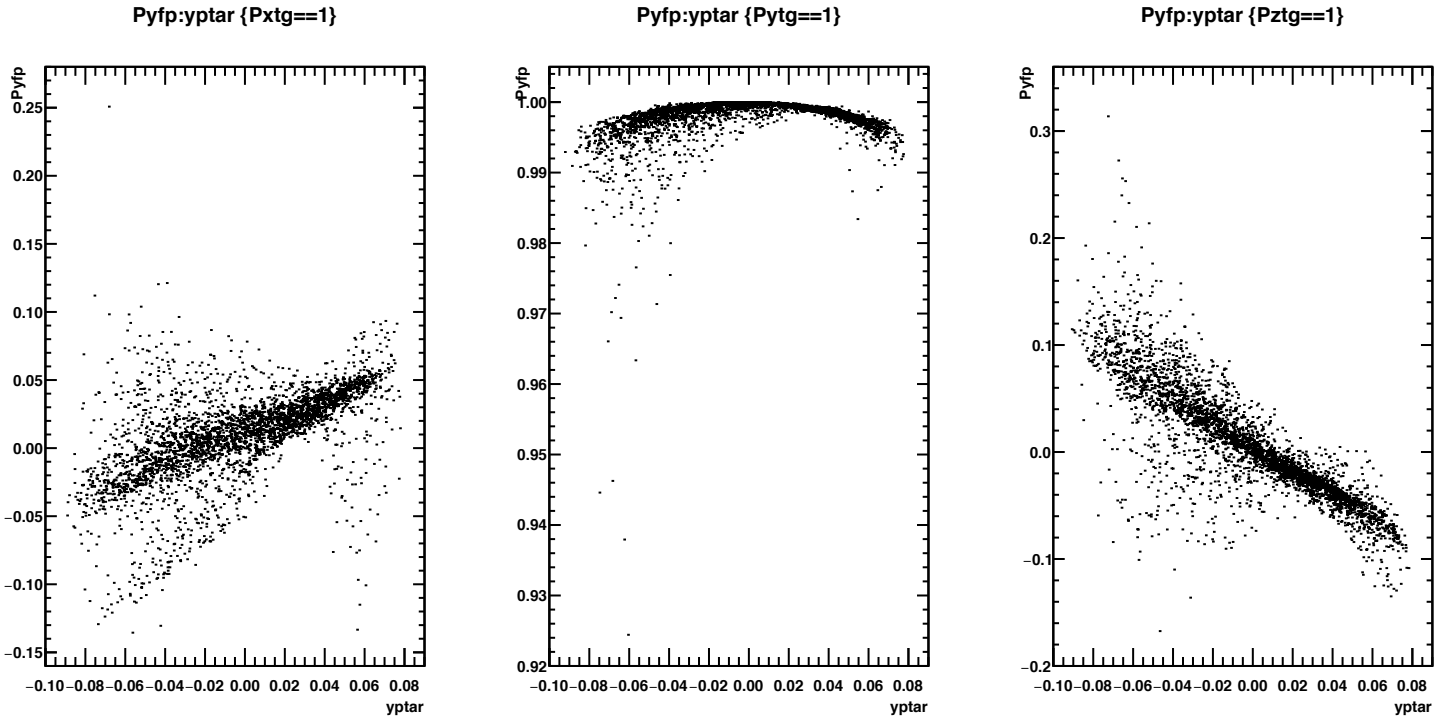

- Non-dispersive-plane precession is non-zero mainly for rays with "yptar" = dy/dz != 0 ("phitarget" in usual Hall A notation)
- S_{yx} has a weak positive correlation with yptar
- S_{yz} (which mixes P_T and P_L), has a stronger negative correlation with yptar
- The slope of this correlation sets the scale for how accurately yptar needs to be determined to achieve a given accuracy on GEp/GMp (no, we haven't done the calculation yet)

Formalism for fitting spin transport matrix elements

- In the usual Maximum-Likelihood analysis, the forward spin transport matrix elements are used. These in turn have to be computed from the reconstructed proton kinematics at the target.
- We expand the "small" deviations from the ideal dipole approximation as a power series in the proton trajectory parameters at the target:
  - xtar, ytar, xptar, yptar, 1/p
- We fit using the SVD as in the case of the optics
- Additional technical challenge:
  - There is no guarantee that if we fit the individual matrix elements without enforcing any constraints, that the 3x3 matrix computed from the resulting expansion coefficients will be a proper rotation for any given event
  - We can try to fit the Euler angle and/or the angle-axis decomposition of the total rotation for a given event, but the problem is that such a decomposition is not unique, and it is difficult to define "good" expansion parameters for such a decomposition.
  - Would like to come up with some kind of constrained optimization procedure to guarantee that the fitted Spin transport coefficients are guaranteed to give a proper rotation in each event.

Spin fit results (5th-order)

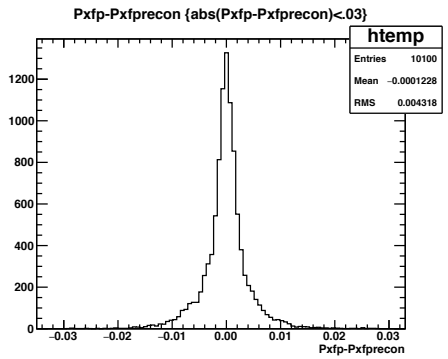

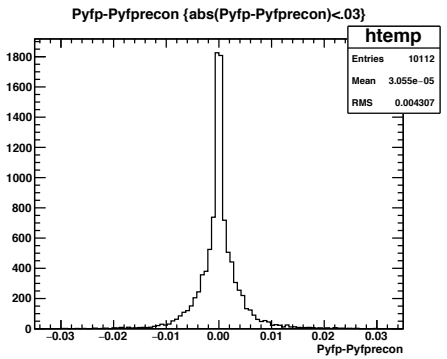

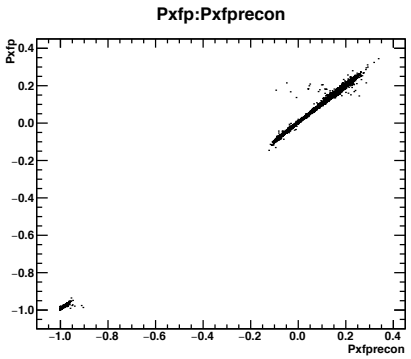

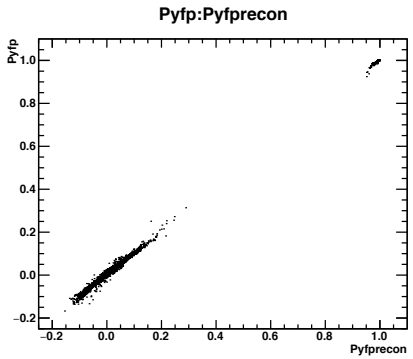

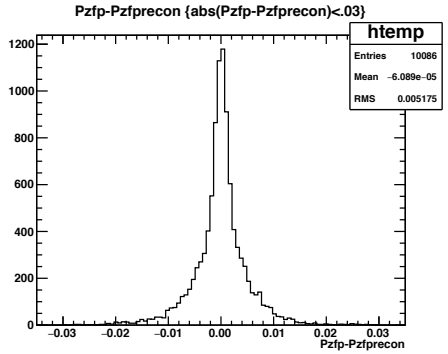

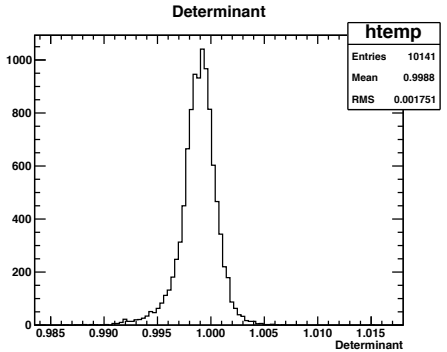

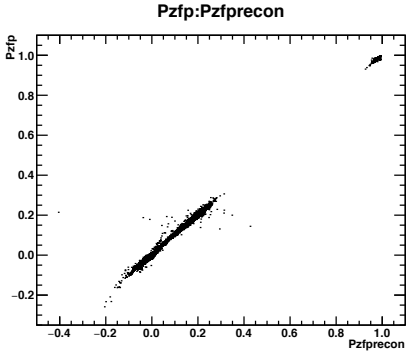

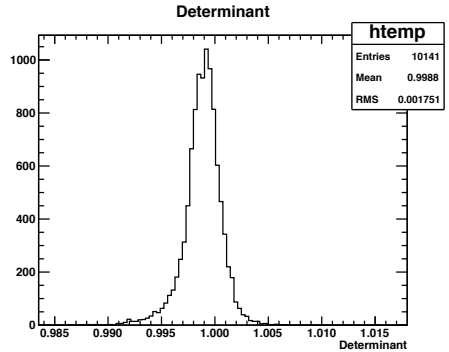

- Fit deviations from the ideal dipole approximation up to 5th-order (still some room for improvement)
- Fit matrix elements directly
- Don’t enforce any constraints
- Determinant results close to 1 in any case.

Final Systematic Uncertainties—Ratio R

Table 3: Systematic uncertainty contributions for $R = -K\frac{P_t}{P_\ell} = \mu_p \frac{G_E^p}{G_M^p}$. The total systematic uncertainty includes the effects of partial correlations among the various systematic contributions, including $\Delta\phi_{tar}$ and Δy_{tar} (correlation coefficient $\rho_{\Delta\phi\Delta y} \approx -0.43$), and $\Delta\theta_{tar}$ and $\Delta\delta$ (correlation coefficient $\rho_{\Delta\theta\Delta\delta} \approx +0.26$). ΔR_{syst}^{total} is the total systematic uncertainty, while ΔR_{syst}^{ptp} is the "point-to-point" systematic uncertainty for $Q^2 = 2.5$ GeV^2 *relative* to the $\epsilon = 0.79$ setting.

Nominal Q^2 (GeV^2)	2.5	2.5	2.5	5.2	6.8	8.5
$\langle\epsilon\rangle$	0.153	0.638	0.790	0.38	0.52	0.24
$\frac{dR}{d\phi_{tar}}\Delta\phi_{tar}$	-3.4×10^{-3}	-2.1×10^{-3}	-2.0×10^{-3}	-4.8×10^{-3}	-5.7×10^{-3}	-0.010
$\frac{dR}{dy_{tar}}\Delta y_{tar}$	-2.6×10^{-3}	-1.2×10^{-3}	-1.2×10^{-3}	-2.9×10^{-3}	-3.9×10^{-3}	-7.7×10^{-3}
$\frac{dR}{d\theta_{tar}}\Delta\theta_{tar}$	-2.2×10^{-3}	-2.5×10^{-3}	-2.5×10^{-3}	1.4×10^{-3}	-5.0×10^{-3}	3.0×10^{-3}
$\frac{dR}{d\delta}\Delta\delta$	5.8×10^{-3}	1.2×10^{-3}	9.0×10^{-4}	1.2×10^{-3}	-3.3×10^{-6}	2.5×10^{-4}
$\frac{dR}{d\varphi_{FPP}}\Delta\varphi_{FPP}$	4.1×10^{-3}	2.5×10^{-3}	2.4×10^{-3}	4.6×10^{-4}	-6.0×10^{-3}	-0.017
$\frac{dR}{dE_e}\Delta E_e$	-1.8×10^{-3}	-1.1×10^{-4}	-5.6×10^{-5}	-1.9×10^{-4}	-8.3×10^{-5}	-1.4×10^{-4}
ΔR_{syst}(background)	3.5×10^{-4}	9.6×10^{-5}	9.9×10^{-5}	2.4×10^{-3}	1.6×10^{-3}	0.012
ΔR_{syst}^{total}	7.9×10^{-3}	4.0×10^{-3}	3.9×10^{-3}	5.5×10^{-3}	9.7×10^{-3}	0.024
ΔR_{syst}^{ptp}	4.3×10^{-3}	2.3×10^{-4}	1.1×10^{-4}	N/A	N/A	N/A

- The precession systematics for the ratio R are more sensitive to non-dispersive-plane offsets of the track position and angles at high Q^2
- In GEp-III, the HMS quadrupoles led to more significant non-dispersive-plane precession and greater mixing of PT and PL within the acceptance than is expected in SBS.
- In GEp-III, dedicated optics studies and careful analysis convinced us that the uncertainty of the total non-dispersive plane trajectory bend angle was ~0.1 mrad.
- In SBS, we probably don't need quite this level of precision due to non-focusing optics, but sensitivity still needs to be evaluated (had an undergrad working on this, who didn't make much progress)